

9-14-2015

# Bridge Weigh-in-Motion Long-term Traffic Monitoring in the State of Connecticut

Valeri I. Kolev  
[valeri.kolev@uconn.edu](mailto:valeri.kolev@uconn.edu)

---

## Recommended Citation

Kolev, Valeri I., "Bridge Weigh-in-Motion Long-term Traffic Monitoring in the State of Connecticut" (2015). *Master's Theses*. 838.  
[https://opencommons.uconn.edu/gs\\_theses/838](https://opencommons.uconn.edu/gs_theses/838)

This work is brought to you for free and open access by the University of Connecticut Graduate School at OpenCommons@UConn. It has been accepted for inclusion in Master's Theses by an authorized administrator of OpenCommons@UConn. For more information, please contact [opencommons@uconn.edu](mailto:opencommons@uconn.edu).

**Bridge Weigh-in-Motion Long-Term Traffic Monitoring  
in the State of Connecticut**

Valeri I. Kolev

B.S., University of Connecticut, 2013

A Thesis Submitted in Partial Fulfillment of the Requirements for the  
Degree of Master of Science at the  
University of Connecticut, September 2015

# **APPROVAL PAGE**

Master of Science Thesis

Bridge Weigh-in-Motion Long-Term Traffic Monitoring in the State of Connecticut

Presented by:

Valeri I. Kolev, B.S.

Major Advisor: \_\_\_\_\_

Shinae Jang, Ph.D

Associate Advisor: \_\_\_\_\_

Richard Christenson, Ph.D

Associate Advisor: \_\_\_\_\_

Sarira Motaref, Ph.D

University of Connecticut, 2015

## **Acknowledgments**

In 2013, towards the end of my undergraduate studies, I made the most significant decision in my professional career. Rather than starting a career in industry, I decided to continue my studies with the goal of strengthening my engineering background in order to handle more challenging structural tasks throughout my career. After two years of hard work, I can say with pride that I have completed a Master of Science degree at the University of Connecticut, and that my abilities have increased exponentially throughout this process.

I could not have completed this degree without help. I would full-heartedly like to thank my major advisor, Professor Shinae Jang, for her mentorship throughout my graduate and undergraduate studies. I would also like to express my gratitude to my co-advisor Professor Richard Christenson, who directed much of my research progression during the latter part of my degree. I similarly would like acknowledge the support of my co-advisor Professor Sarira Motaref who assisted me much with my thesis work.

Furthermore, I wish to express my gratitude to Anne-Marie McDonnell for her support of my research project and for her guidance. My thesis would not have been possible has it not been for the Connecticut Department of Transportation, the organization having financially supported my research through project SPR-2290. I would like to express my deepest gratitude to my friends and colleagues; Edward Eskew, Rosana Martinez-Castro, Colin (Chenhao) Jin, Kelly Bertolaccini, Sergio Lobo-Aguilar, Michael Harris, Masoud Mehrraoufi, Dominic Kruszewski, Suvash Dhakal, Surendra Baniya, Jason Henion, and Amanda McBride. Their support has been instrumental in the complication of my degree. Finally, I would like to thank my family for their continuous backing throughout my education.

## Table of Contents

<b>CHAPTER 1.INTRODUCTION.....</b>	<b>1</b>
1.1 MOTIVATION OF TRAFFIC LOAD ANALYSIS.....	1
1.2 LIVE LOAD MODEL BASED ON TRAFFIC DATA .....	2
1.3 BRIDGE WEIGH-IN-MOTION .....	4
1.4 IMPACT OF THE RESEARCH .....	5
1.5 THESIS OUTLINE.....	7
<b>CHAPTER 2.LITERATURE REVIEW .....</b>	<b>8</b>
2.1 BRIDGE WEIGH-IN-MOTION .....	8
2.1.1 <i>COST323 and WAVE Programs</i> .....	9
2.1.2 <i>Recent Studies in BWIM</i> .....	10
2.1.3 <i>BWIM Research in Connecticut</i> .....	11
2.2 RELIABILITY STUDIES IN LOAD ESTIMATION.....	12
2.2.1 <i>AASHTO Design Methodology</i> .....	13
2.2.2 <i>State Specific Calibration Methods</i> .....	14
2.2.3 <i>Load Estimation based on Strain Measurements</i> .....	15
<b>CHAPTER 3.FULL-SCALE EXPERIMENTAL VALIDATION.....</b>	<b>17</b>
3.1 TEST BED DESCRIPTION: MERIDEN BRIDGE .....	17
3.2 SHM-BWIM SYSTEM .....	19
3.3 DYNAMIC TRUCK LOADING TESTS.....	21
3.4 LONG-TERM DATA COLLECTION .....	22
3.5 BWIM METHODOLOGY .....	24
3.5.1 <i>Gross Vehicle Weight</i> .....	24
3.5.2 <i>Vehicle Speed Estimation</i> .....	25
<b>CHAPTER 4.BRIDGE WEIGH-IN-MOTION RESULTS .....</b>	<b>28</b>
4.1 TEST TRUCKS SPEED CALCULATION .....	28
4.2 FREE FLOWING TRAFFIC.....	31
4.2.1 <i>Trucks Travelling during Traffic Jams</i> .....	32
4.2.2 <i>Lane Changes</i> .....	33
4.2.3 <i>Multiple Presences</i> .....	35
4.2.4 <i>Extensive Accelerations or Unusual Vehicle Configurations</i> .....	37
4.2.5 <i>Light Vehicles</i> .....	38
4.3 FREE FLOWING TRAFFIC EVALUATION.....	40
4.4 STATISTICAL EVALUATION OF THE ALGORITHM.....	40
4.5 FREE FLOWING TRAFFIC FINAL RESULTS.....	42
4.6 LONG-TERM TRAFFIC RESULTS .....	44
4.6.1 <i>Type of Data Collected</i> .....	45
4.6.2 <i>Monthly Speed</i> .....	45
4.6.3 <i>Speed Calculation: February 2015</i> .....	47

4.6.4	<i>Speed and GVW Calculation for February 13<sup>th</sup>, 2015</i>	48
4.6.5	<i>Average Daily Truck events</i>	52
4.6.6	<i>Speed Errors</i>	53
4.6.7	<i>Temperature Effects on Algorithm Accuracy</i>	57
<b>CHAPTER 5. RELIABILITY STUDY RESULTS</b>		<b>59</b>
5.1	TEST TRUCK RESULTS	59
5.2	MAXIMUM MOMENT CALCULATIONS	61
5.3	STATISTICAL PARAMETERS	62
5.3.1	<i>Dead Load Statistical Parameters</i>	62
5.3.2	<i>Moment Resistance Statistical Parameters</i>	63
5.3.3	<i>Extreme Type I Modeling for Live Loads</i>	63
5.4	FINAL RESULTS	65
5.4.1	<i>Dynamic Load Statistical Parameters</i>	66
5.5	STUDY APPLICATION	67
<b>CHAPTER 6. CONCLUSIONS AND FUTURE WORK</b>		<b>69</b>
6.1	BWIM	69
6.1.1	<i>BWIM Summary and Conclusions</i>	69
6.1.2	<i>BWIM Future Studies</i>	70
6.2	RELIABILITY STUDY	71
6.2.1	<i>Live Load Calibration Study Summary and Conclusions</i>	71
6.2.2	<i>Future Studies of Live Load Calibration</i>	72
<b>REFERENCES</b>		<b>74</b>

## List of Figures

Figure 3.1: East elevation of the Meriden Bridge Northbound.....	18
Figure 3.2: Meriden Bridge plan view .....	18
Figure 3.3: Schematic of sensor layout and types .....	19
Figure 3.4: Cabinet containing Meriden Bridge system components.....	20
Figure 3.5: Test truck used in calibration.....	21
Figure 3.6: Girder 6 strain responses during two minutes.....	22
Figure 3.7: Typical strain response due to a five axle truck .....	26
Figure 3.8: Typical five axle truck .....	27
Figure 4.1: Lane 1 strain response of a truck during traffic .....	32
Figure 4.2: Five axle truck during traffic .....	33
Figure 4.3: Lanes 1 and 2 strain response of a truck changing lanes .....	34
Figure 4.4: Five axle truck changing lanes.....	34
Figure 4.5: Lane 1 strain response of a multiple presence event .....	36
Figure 4.6: Multiple presence event .....	36
Figure 4.7: Lane 1 strain response of an irregular vehicle .....	37
Figure 4.8: Irregular vehicle .....	38
Figure 4.9: Lane 1 strain response of a light vehicle .....	39
Figure 4.10: Light vehicle .....	39
Figure 4.11: Lane 1 traffic speeds .....	50
Figure 4.12: Lane 2 traffic speeds .....	50
Figure 4.13: Lane 1 GVWs.....	51
Figure 4.14: Lane 2 GVWs.....	51
Figure 4.15: Truck followed closely by light vehicle, Error Type I.....	54
Figure 4.16: Truck record not captured by algorithm, Error Type II .....	54

Figure 4.17: Temperature and GVW correlation .....	57
Figure 5.1: $(\beta_{\text{resulting}} - \beta_{\text{target}})^2$ vs. Live Load Factor using all data.....	66
Figure 5.2: $(\beta_{\text{resulting}} - \beta_{\text{target}})^2$ vs. Live Load Factor using May, 2014 data .....	66

## List of Tables

Table 3.1: Percentages of data collected per month.....	23
Table 4.1: Lane 1 test truck speed calculations.....	29
Table 4.2: Lane 2 test truck speed calculations.....	29
Table 4.3: Lane 1 test truck GVW calculations .....	30
Table 4.4: Lane 2 test truck GVW calculations .....	31
Table 4.5: Percentage GVW difference for free flowing traffic .....	42
Table 4.6: GVW difference for free flowing traffic in kips.....	43
Table 4.7: 95% confidence interval accuracy .....	43
Table 4.8: Monthly speed data.....	46
Table 4.9: Average speeds per day for February 2015 .....	48
Table 4.10: Average Daily Truck Traffic .....	53
Table 4.11: Average percent errors.....	55
Table 4.12: Error types for the month of February 2015 .....	56
Table 5.1: Strain Responses from a Test Truck in travelling in Lane 1.....	60
Table 5.2: Strain Responses from a Test Truck travelling in Lane 2.....	61
Table 5.3 Dead Load statistical parameters .....	63
Table 5.4: Moment Resistance statistical parameters .....	63



## **CHAPTER 1.INTRODUCTION**

### **1.1 Motivation of Traffic Load Analysis**

Proper management and maintenance of the road transportation network is of great value to the economy of United States, as it is a critical link of transporting people and goods throughout the country. This task is becoming more challenging with the aging of the highway network and the nation's bridges, as well as the increase in freight transportation. According to the American Society of Civil Engineers (ASCE) 2013 Annual Report Card, 32% of America's major roads have a poor or mediocre pavement condition. As a result of this, 67 billion dollars were spent by motorist on vehicle repairs and operating costs (ASCE, 2013). The performance of the nation's bridges is directly tied into the health of the transportation network. In 2013, 24.9% of bridges in the United States were classified as either structurally deficient or functionally obsolete. According to the Annual Report Card, current government funding is not sufficient to keep up with the deterioration of roads and bridges, which is why it is of great importance to optimize management and maintenance decisions.

A key to preservation of the nation's transportation network is gathering reliable traffic data. In recent years, data-driven decisions for infrastructure maintenance have been encouraged by the Federal Highway Administration (FHWA), American Association of State Highway and Transportation Officials (AASHTO), and the Transportation Research Board (TRB) (Strocko, 2013). Useful information for decision making includes truck weights, types, and number of trucks travelling on the highway network, as well as the corresponding time of day for such occurrences.

Currently, such data can be collected at weigh stations, which require trucks to pull over and be weighed statically. Further methods include using Weigh-in-Motion (WIM) technologies

which use in-pavement sensors to collect vehicle and axle weights of truck traffic travelling at low or highway speeds. An alternative to traditional weigh stations and WIM systems is Bridge Weigh-in-Motion (BWIM), the process by which gross vehicle weights (GVW) and axle weights can be determined for trucks travelling over highway or regular bridges instrumented with sensors (UTCA, 2012). The first major part of this study will focus on a BWIM system in the state of the Connecticut.

Many of the bridges in Connecticut and in the Northeast of the United States have complications with corrosion of steel girders and other bridge components, which result from exposure to chloride ions from de-icing vehicles. Inspections performed every two years require that load ratings be performed if conditions of the primary members of the bridge have experienced significant change since the previous inspection (FHWA, 2012). Load ratings are intended to measure live load capacity of bridges and such measurements are performed using Load and Resistance Factor Design (LRFD) rating factors. However, these factors are intended for the entire country and for all bridge types and configurations. Calibration of the live load factors from local traffic can allow bridge municipalities to make better decisions when determining if the integrity of a bridge is affected from damage or corrosion. The second part of this master's thesis focuses on calibrating the live load factor in the AASHTO LRFD Strength I Limit State equations in order to make them more applicable to the state of Connecticut. The study is performed using strain responses collected from an in-service BWIM system.

## **1.2 Live Load Model based on Traffic Data**

Many decisions made regarding infrastructure management, such as configuration and amount of freight trucks passing over the network, are based on approximations and assumptions

(Christenson, 2014). In most cases historical data is used, while local and recent data is rarely available. For example, the AASHTO LRFD Bridge design specifications, which are used throughout the United States today, were created through a research project in the 1970s based on traffic over a bridge in Canada (Nowak, 1999). Accurate new weight data gathered from WIM and BWIM systems can be used for improvements in pavement and bridge design, load rating analyses, and overweight vehicle identification. Furthermore, freight traffic information can be used by municipalities to assist with funding allocation decisions, by providing an alternative way to determine which highways are most critically travelled.

The primary function of pavement is load distribution of the tire loads. Pavement design decisions are based on factors such as tire axle loads, axle and tire configurations, load cycles, and vehicle speed, information which can be better identified using accurate truck traffic data. Local traffic information can allow for better decision in pavement design and management.

Bridge design decisions and load rating analysis can similarly be improved. Multiple studies have been performed across the United States to calibrate the AAHSTO LRFD Live Load factors using local traffic data (Kwon et al., 2009; Fu and van de Lindt, 2006). These studies can directly be used to better understand how much extra capacity bridges have, by comparing traffic patterns used to calculate the original calibration factors and local traffic patterns. Furthermore, fatigue and fracture limit state of bridges is defined in term of stress-range cycles and the number of cycles can be better estimated given accurate traffic information.

Overweight trucks can contribute to pavement failure by increasing pavement wear and bridge fatigue damage (Jacob et al., 2010). According to the South Dakota Department of Transportation, in exceeding the legal axle weight limit by more than 20% the pavement life consumed will be more than two times greater than that of an axle weight at legal limit (SDDOT,

2003). When truck loads exceed maximum limits, there can be an increased risk of a traffic accident that can be caused by truck instability, braking system damage, tire blowout, or loss of maneuverability (Jacob et al. 2010). Collection of BWIM data can be useful in identifying which trucks should potentially be weighed more accurately, or for weigh station scheduling. Current methods are not accurate enough for direct enforcement.

### **1.3 Bridge Weigh-in-Motion**

In the United States, traditional weigh stations are commonly used to weigh trucks to collect traffic information and ensure drives comply with safety regulations. One priority of weigh station is to identify overweight trucks. Weigh stations are checkpoints along highways equipped with static trucks scales or low speed WIM systems. A signal light is commonly used to indicate to truck drivers that they must pull into the station to be weighed. Though the weigh station can provide accurate information about truck weights, it requires staff and time perform each weighing, which can be ineffective with heavy traffic flow, and the station can be congested resulting in an time punishment for overweight and compliant trucks (Jacob et al, 2010). When truck volume begins to exceed weigh station capacity, violators can bypass the stations and compromise the effectiveness of the system (Lee et al, 2009). Furthermore, truck drivers can effectively communicate amongst each other to avoid open stations.

Data can be collected at highway speeds using Weigh-in-Motion (WIM) technologies which use in-pavement sensors to collect weight details of truck traffic. However, these types of systems have limitations which include the risk of workers during installation, dependencies of the sensors on pavement conditions, influence of vehicle dynamics to the accuracy of the system, and susceptibility of sensors to damage (Christenson, 2014).

BWIM has the potential to overcome many of the shortcomings of weigh stations and WIM systems, and to provide long-term traffic monitoring option for agencies responsible for highway infrastructure maintenance. BWIM systems can utilize different sensor technologies and, using the vibration data of bridge components, estimate the desirable vehicle information. BWIM practices have been developed as a non-intrusive approach, where no sensors are placed in the pavement, but instead are installed on the underside of the bridge (Wall et al, 2009). These are also known as Nothing-On-The-Road (NOTR) or Free-of-Axle Detector (FAD) technology. However, BWIM schemes still have some drawbacks in less accuracy during the presence of multiple trucks, while trucks are changing lanes, and during traffic delays, as well as under certain bridge spans and skews (COST 323, 2002; UTCA, 2012). Therefore, BWIM systems are not ideal for every highway bridge and selection of instrumentation should be carefully considered.

#### **1.4 Impact of the Research**

In this master's thesis, results are presented involving analysis of strain measurements gathered from an existing BWIM system installed on a single-span, steel girder bridge, located on Interstate 91 in Meriden, Connecticut. A BWIM algorithm has been used to calculate GVWs and speeds of trucks passing over the bridge using strain responses from steel girders. A new truck speed calculation method was developed and demonstrated strong potential. The methodology is validated using two sets of data; a test truck of known weight travelling over the bridge at known speeds and a set of trucks from free flowing traffic that were weighed at a near-by weigh station. The method is further applied to a long-term set of data consisting of more than one year's worth of strain responses collected continuously (24/7). Final results include information regarding the

accuracy of algorithm and comprehensive information on the weight of trucks travelling over the bridge for the period of close to one year.

In past research studies, only short-term data has been used for GVW and speed estimations from either calibration vehicles or free-flowing traffic, while truck traffic for long periods have not been examined. This research study provides a unique opportunity to observe how a BWIM system performs when examining long-term data and what benefits and challenges exists with such collection.

The long-term traffic data collected from the BWIM system provides a unique opportunity to quantify the weight of local trucks travelling in the state of Connecticut. A study is conducted to use this information in order to calibrate the live load factor in AASHTO LRFD Design Specifications using local traffic. Maximum moments are determined from strain data of two interior girders of the bridge, which are assumed to be most critical. Past research performed on calibrating design codes using local traffic has been conducted using data from WIM system, which provide vehicle GVWs and configurations that can be virtually placed on a bridge of interest. However, most type of live load uncertainties, due to dynamic, multiple presence of vehicles, or girder distribution factors, are not taken into account through WIM data. By using strain responses from BWIM systems, vibration responses directly from girders are used, therefore many of the uncertainties in the AASHTO LRFD Design Specifications are accounted for. Furthermore in this study, statistical parameters regarding the dead loads, live loads, and moment resistance of the bridge, as well assumptions regarding the distribution types for each variable are gathered from previous research. New statistical parameters for live loads are established using the collected strain responses. A Monte Carlo simulation is used in order to define a new optimum live load factor. Finally, a new method of establishing a ratio between

girder moment and strain allows for the application of this new live load factor to other bridge types across the state.

## **1.5 Thesis Outline**

This master's thesis is organized in a total of seven chapters. Chapter 1 provides an introduction and motivations behind BWIM research, as well as details on the studies presented. Chapter 2 contains a literature review on the topic of BWIM that includes history as well as recent developments in the field. Furthermore, Chapter 2 contains a literature review of reliability based methods used to calibrate AASHTO LRFD Design Specifications based on local traffic data, as well as studies using bridge responses for relevant purposes. Chapter 3 presents the current BWIM system installed on the Meriden Bridge, including methods of instrumentation, location and sensor types. The post-processing of the data is also discussed in this chapter. Chapter 4 explains the BWIM methodology and contains the results in this research study, including the validation of the speed and GVW calculation methodologies and processed data for close to one year worth of strain responses. Chapter 5 focuses on the separate study presented, which entails the calibration of the live load factor in AAHSTO LRFD codes using data from the BWIM system. This chapter includes statistical parameters for dead loads, live loads, and moment capacity of the Meriden Bridge. In addition, Chapter 5 contains results from a Monte Carlo simulation and a discussion. Finally, Chapter 6 covers conclusions and applications of both research projects presented.

## **CHAPTER 2. LITERATURE REVIEW**

This chapter provides a comprehensive literature review on the topic of BWIM including the history of this topic, advance studies performed in Europe, current and more recent research, and BWIM projects in the state of Connecticut. In addition, a reliability based literature review is presented discussing the history of the current AASHTO LRFD design codes and various studies relevant to research performed in this master's thesis.

### **2.1 Bridge Weigh-in-Motion**

Bridge Weigh-in-Motion was first proposed in the late 1970s by Moses (Moses, 1979). Moses combined traffic and strain sensors installed on the pavement and the highway bridge girder, respectively. In his study, the traffic sensors were used to determine the vehicle speeds and axle spacing, while the strain sensors were used to compare strain data to influence lines determined from a bridge model.

In 1999, O'Brien improved the testing process by requiring a theoretical influence line as opposed to an actual influence line. The theoretical influence line could be scaled up or down based on a calibration truck (O'Brien et al, 1999). A more recently created procedure by Ojio and Yamada (2002) was used to determine GVW without the need for an influence or theoretical line. This method involves the integration of strain response data, combined with a speed adjustment and a calibration factor, to determine the GVW (Ojio and Yamada, 2002). The calibration factor is determined from a test truck passing over the bridge.



### **2.1.1 COST323 and WAVE Programs**

In Europe, extensive research into Weigh-in-Motion (WIM) systems was performed in the late 1990s as part of the COST323 and WAVE programs. COST323 was the first European cooperation on WIM. This study produced reports concerning the needs for a specification of WIM systems, a glossary of terms, a European database, large scale common tests of various systems, and two conferences (Quilligan, 2003). The research study also developed criteria regarding the optimal bridge selection to use a BWIM system. The optimal length of the bridge section which influences the instrumentation should be between 5 and 15 meters (16.4 and 49.2 feet), while an acceptable length is between 8 and 35 meters (26.2 and 114.9 feet) (COST 323, 2002). The study also suggested an optimal bridge skew of less than 10 degrees, and an acceptable bridge skew of less than 25 degrees (COST 323, 2002). A further benefit of this study was a classification system for WIM accuracy that is based on percentage of gross vehicle weight difference between estimated and actual GVW. The accuracy class letters of A, B+, B, C, D+, and D correspond to an GVW percent accuracy of  $\pm 5$ ,  $\pm 7$ ,  $\pm 10$ ,  $\pm 15$ ,  $\pm 20$ , and  $\pm 25$  for a 95% confidence interval, respectively.

Due to considerable demand for more accurate WIM systems in Europe, a proposal for a large research project emerged. Known as “Weigh in motion of Axles and Vehicles for Europe,” or WAVE, this project began in 1996 and lasted until 1999, involving a total of 11 researchers from 10 different countries (WAVE, 2001). The general objectives of this study were to improve the accuracy of traditional WIM systems, extended WIM to different types of bridges, test WIM systems in cold regions, and improve calibration procedures. As a result of this extensive study, a new approach was developed for a system that requires no axle detector on the road surface with

this system achieving good accuracy. Additionally, the study developed a Quality Assurance system of WIM and two new algorithms for Multi-Sensing WIM.

During the WAVE project, Slovenia's National Building and Civil Engineering Institute (ZAG) developed a BWIM system known as SiWIM. This NOTR or FAD system uses a series of strain transducers instrumented below the bridge in order to determine a vehicle's axle weight, axle spacing, speed, class, and GVW (UTCA, 2012).

### **2.1.2 Recent Studies in BWIM**

A recent application of the BWIM system was performed in Alabama using the commercially available SiWIM system. In 2007, the University Transportation Center for Alabama worked on the first CESTEL SiWIM system in the United States (UTCA, 2012). The objective of the research study was to evaluate the potential use of the SiWIM BWIM system in Alabama. Over an 18 month period, two interstate bridges in the state of Alabama were instrumented with the system and calibrated using trucks of known weight. The conclusions of the study resulted in many field study recommendations, such as using bridges with two lanes or less, selecting a bridge with no skew, and to use fully loaded test vehicles (UTCA, 2012).

A comprehensive study by the Virtual Vehicle Competence Center in Austria has explored different methods for detecting vehicle data using BWIM systems. Data was used from SHM systems installed on three different bridges in Austria (Pircher et al, 2008). Based on this research a method for detection of vehicle velocity, axle weights, axle spacing, and number of axles has been explored using wavelet analysis and optimization procedures (Lechner et al, 2013). The study further explored using statistical approaches and regular vehicle information to calibrate BWIM systems rather the use of trucks of known weight and configuration, which have

been commonly used in these studies. Past research from this institution has calculated velocities of trucks by using wavelet decomposition and obtaining the difference between the first and last axle of a truck (Lechner et al, 2010).

In Europe, a research project lead by four SMEs (Small and Medium Enterprises) from multiple European countries has been conducted with the goal of improving BWIM systems (Bridgemon, 2015). Partners of this project include ZAG and CESTEL as well as other institutions. This project involved testing of three bridges in Slovenia including a box culvert and two concrete girder bridges (O'Brien, 2014). The study focused on improving accuracy of BWIM systems by taking bridge vibrations into account, calibrating the system for temperature changes and dynamic effects from speeds, enhancing axle detection using wavelets signal processing methods and improving data quality assurance using statistical methods (O'Brien, 2014). This project was completed in 2015 and detailed results are yet to be released (Bridgemon, 2015).

### **2.1.3 BWIM Research in Connecticut**

In 2004, work began on the application of BWIM systems in the state of Connecticut. A field test was performed in 2006 on an already monitored multi-span steel girder bridge in Connecticut, which demonstrated that a BWIM system can be created using an existing bridge monitoring system (Cardini and DeWolf, 2007). In November 2008, a field test was performed where strain sensors from a portable system were installed on a single-span, steel girder bridge located in Meriden, Connecticut (Wall et al, 2009). The bridge contained promising characteristics for instrumentation including short span, little skew, and a good structural condition. Using a test truck of known weight and a known travelling speed the GVW accuracy of the system was found

to be +6.31 / -6.31% for the slow lane, +15.20 / - 15.19% for the central lane, when comparing estimated and actual GVWs. Accuracy of the algorithm from free flowing traffic was examining 117 trucks for a 95% confidence interval was found to be +23.39 / -27.28% for the slow lane and +51.70 / -39.23% for the middle lane. As a result of these studies a research project SPR-2265 was developed and a dual purpose BWIM and Structural Health Monitoring (SHM) system was installed on the mentioned bridge.

The study presented in this master's thesis enhances the research performed in Connecticut. In August of 2014 a new project has been funded by the Connecticut Department of Transportation (CTDOT) and the Federal Highway Administration (FHWA), known by the name "Advancing the State of Bridge Weigh-in-Motion for the Connecticut Transportation Network." This project has the aim to collect continuous BWIM data from the Meriden Bridge making improvements to the calculations of speeds and GVWs of trucks. Furthermore, the project aims to develop a new BWIM system that can be temporarily or permanently installed on a bridge of interest. Different types of bridges will be instrumented with the system, and may include concrete or box girder bridges, and bridges with large slope, skew, or long-spans.

## **2.2 Reliability Studies in Load Estimation**

In recent years, bridge design practices have been moving away from Allowable Stress Design (ASD) and Load Factor Design (LFD) to Load and Resistance Factor Design (LRFD) design methods. The FHWA requires that all bridges designed after October 2007 to use the AASHTO LRFD Design specifications (Kwon et al, 2009).

### **2.2.1 AASHTO Design Methodology**

The basis of the AASHTO LRFD design methodology comes from the NCHRP Report 368 (Nowak, 1999). The research discussed in the report was conducted in the mid-1970s. At this time, there was no available truck data in the United States required for the study and as a result data was used from a bridge in Ontario, Canada. Heavy trucks traveling on this bridge virtually placed on various types of bridges in the United States and design factors were proposed in AASHTO LRFD design equations. Based on the survey data a suggested live load factor of 1.70 was determined. This factor was increased to 1.75 to account for the significantly larger Average Daily Truck Traffic (ADTT) of 5,000 expected on United States highways when compared with the remote surveyed site, 1,000. The LRFD code aims for the reliability factor of 3.5 which equates to 2 failures in 10,000 cases.

The dead load parameters used in Nowak (1999) are based off NBS Report 577, which consider three different types of dead loads including: factory-made members (steel, precast concrete), cast-in-place members (concrete), wearing surface (asphalt), and weight of miscellaneous item (Nowak, 1999). Each of these different dead load components has a unique bias factor and coefficient of variation.

In order to determine effects on the bridge from live loads, a survey was carried out in which 9,250 heavy trucks were used to calibrate the live load factor (Nowak, 1999). Vehicles from this survey were virtually run over the influence lines of different bridge configurations to determine maximum loadings. A normal probability plot was used to predict long-term truck loads based on short-term records. This data was applied to close to 200 existing bridges in the United States, with a variety of geometric configurations, material properties, and bridge types.

The resistance of a bridge can be treated as a Random Variable (R.V.) with randomness caused by material properties, fabrication tolerances, and professional assumptions. Each source of uncertainties will have a unique mean and standard deviation. In report NCHRP 358, the majority of properties have been treated as a normal distribution except the yield of steel, which was deemed to follow a lognormal distribution.

Report NCHRP 20-7/186 documented the calibration of the AASHTO LRFD Strength Limit State and clarified parameters for dead load, live load, and resistance parameters (Kulicki, 2007). The study recommended that future work should be conducted using Monte Carlo simulation rather than the Rackwitz and Fiessler procedure used in the original calibration report.

### **2.2.2 State Specific Calibration Methods**

Since the original calibration results in NCHRP Report 368, research studies have been used to calibrate the design codes based on local traffic data from specific states.

The Missouri Transportation Institute and Missouri Department of Transportation studied the live load factor in the Strength I Limit State equation in AASHTO based on WIM data specifically gathered from the state of Missouri (Kwon et al, 2009). The study compared using a normal probability plot and Gumbel Type I distribution in order to simulate expected 75-year maximum loads effects, concluding that the latter method provides more consistent and conservative values (Kwon et al, 2009). The report found that the majority of bridges examined had reliability value higher than the optimal value, and recommended that a factor of 0.95 be applied to the existing factor for bridges with an Average Daily Truck Traffic (ADTT) between 2,500 and 1,000, and that a factor of 0.90 be applied to bridges with an ADTT less than 1,000.

A study conducted by the Michigan Department of Transportation explored what scaling of the AAHSTO LRFD code would allow for reliability index consistent with current regulations (Fu and van de Lindt, 2006). Live Loads were projected assuming a single truck case for the calculation of the GDF and an application of an impact factor. Data sets of WIM data were run over selected bridges in the state. Dead load and bridge capacity factors were found consistent with report NCHRP 368 and used in this study. A twenty percent increase of the current live load factor was proposed for critical regions of state and no further modifications were suggested for applications to the code.

### **2.2.3 Load Estimation based on Strain Measurements**

Multiple studies have been performed using strain response directly from bridge components for various purposes. Using measurements directly from bridge components eliminates uncertainties in bridge design codes due girder distribution, multiple presences of vehicles, and impact factors. Therefore, such measurements can lead to more accurate predictions of the bridge's integrity.

Through a system installed on a three-span continuous, steel girder bridge in Delaware a study was performed where over a period of 11 days, truck events were registered when exceeding a strain value (Bhattacharya et al, 2005). The maximum truck effects on the bridge were modeled using a Gumbel distribution and results indicated that varying the exceeding value does not change the extreme values greatly and the coefficient of variation for the live load effect varied between the values of 10% and 13% (Bhattacharya et al, 2005). As a continuation of this study the maximum 75 year moment due to single presence and multi presence of vehicles were compared with the HL-93 loading and it was determined that the moment found by the HL-93 system was close to 3.5 times greater than the one predicted from in service data (Guzda, 2007).

Other relevant studies were used to analyze the performance of current bridges. A field study was conducted on a damaged steel girder bridge in Vermont, and through nondestructive testing it was concluded that bridge repairs were not necessary due to an alternative load path which developed in the superstructure (Brena, 2013). In a separate project, a load rating of an existing bridge was computed using a finite element model (FEM) and result were compared with load rating factors calculated from standard AASHTO LRFD methods (Bell et al, 2013).



## **CHAPTER 3. FULL-SCALE EXPERIMENTAL VALIDATION**

In this chapter, details are presented regarding the Meriden Bridge, which is the test bed for this research. The information presented includes dimensions and characteristics of the bridge, as well as sensors locations, types, and parameters. In addition, details of three separate data sets are included. The first set of data is composed of vibration responses from a test truck travelling over the bridge. Characteristics such as GVW, axle weights, axle spacing, and speeds are known for this vehicle. The second set of data entails free flowing truck traffic, the vibration responses of which have been recorded and matched with vehicles that were weighted using a static scale. The third set of data relates to 385 days of collected vibration data. The methodology behind the algorithm is presented in this chapter, including the calculations used for GVW and speed estimations.

### **3.1 Test Bed Description: Meriden Bridge**

The test bridge used in this study is a three-lane bridge which carries Interstate 91 (I-91) Northbound over Baldwin Avenue. It is located in Meriden, Connecticut and has the Bridge No. 03051. As was discussed previously, the length and skew of the bridge can significantly contribute to the accuracy of a BWIM system. This bridge has a total length of 85 ft., a width of 55 ft., and a bridge skew of  $11.5^\circ$ , which falls in the recommended COST323 category for length and acceptable COST 323 category for skew (COST, 2002). According to CTDOT, the bridge carries an average daily traffic of 57,000 vehicles with 7% of those being trucks (Li, 2014). This results in average daily truck traffic (ADTT) of 4,000. A photo of the east elevation of the bridge can be seen in Figure 3.1.



**Figure 3.1: East elevation of the Meriden Bridge Northbound (Wall *et al*, 2009)**

An inspection of bridge was performed on September 24, 2012 by HAKS Engineers (HAKS, 2012). The bridge received a sufficiency rating of 95 out of 100, where a rating of 100 is entirely sufficient. According to Wall, 2009 the Meriden Bridge received a rating of 96 out of 100 from an inspection performed on August 12, 2009 (Wall *et al*, 2009). From these reports it can be concluded that there have been no significant changes to the structural integrity of the bridge in the past four years. Both ratings are satisfactory for the bridge to remain in service.

Figure 3.2 shows the dimensions of the bridge.

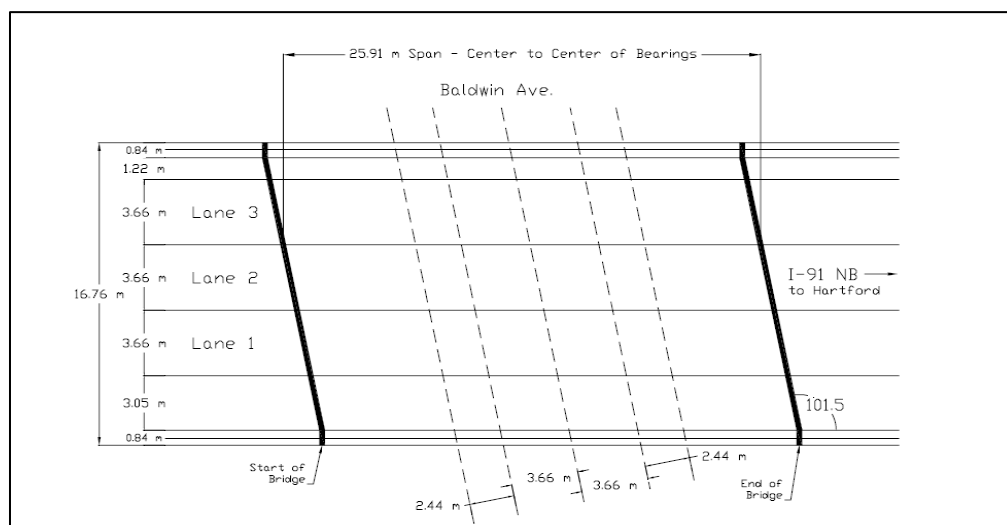


**Figure 3.2: Meriden Bridge plan view (Wall *et al*, 2009)**

### 3.2 SHM-BWIM System

A dual Structural Health Monitoring (SHM) and BWIM system has been instrumented on the Meriden Bridge. A total of 38 sensors have been installed on the bridge including 18 foil strain sensors, 4 high sensitivity quartz strain transducers, 8 piezoelectric accelerometers, 4 capacitive accelerometers, 4 resistance temperature detectors, and one microphone. Figure 3.3 shows the configuration of the various sensor technologies.

For the purpose of this study only two strain sensors have been used, located at the center of Girders 4 and 6. Both sensors are installed on the web of the girder, just above the bottom flange and measure vertical strain. Girders 4 and 6 are located almost directly under the slow and middle lane of the highway, respectively. The Meriden Bridge has a total of three lanes; however, very few trucks are known to travel in the far left (fast) lane. As a result, data was only collected for the right and middle lanes. It was expected that the girders discussed will experience the greatest strain measurements from each corresponding lane at the mid span of the bridge. Hence, the middle lane will be referred to as Lane 2 and the slow (right) lane as Lane 1.

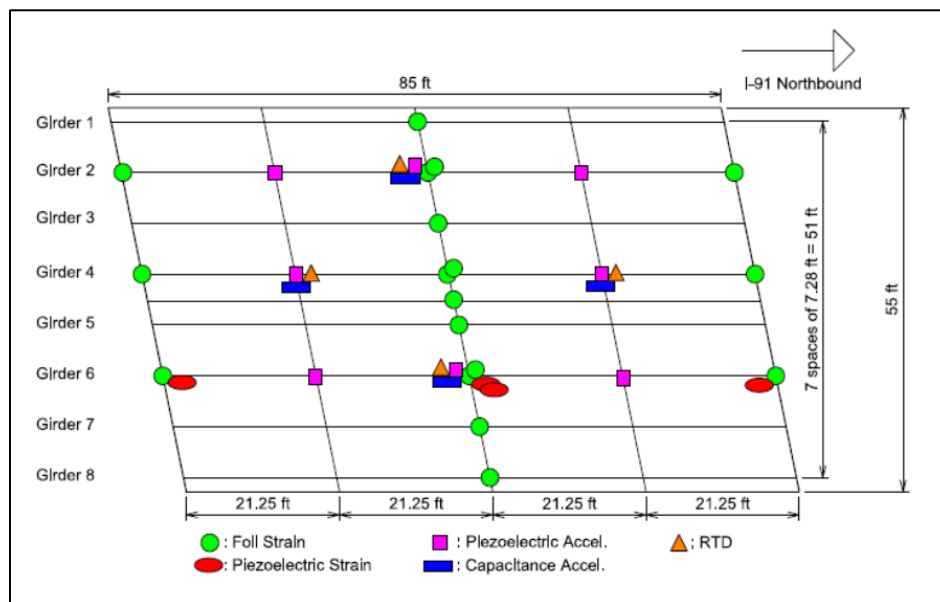


Figure 3.3: Schematic of sensor layout and types (Christenson *et al*, 2012)

Only foil strain sensors are used in the research presented and will be discussed in more detail. These types of strain sensors are commonly used for the purposes of bridge monitoring. The specific sensors used in this study are manufactured by Vishay Micro-Measurements and they have a measurement range of 1000s of microstrain, while the greatest peaks observed on the bridge have been less than 50 microstrain.

The data acquisition unit used is a National Instruments (NI) NI cDAQ-9178 CompactDAQ with four different types of modulus used for different sensor types (Li, 2014). The DAQ unit is connected to a small desktop using a USB 2.0 High-Speed Cable (Li, 2014). The configuration described is placed inside a traffic signal cabinet that is installed on the south abutment of the Meriden Bridge. Figure 3.4 shows an image of the cabinet. The desktop contains the programming language MATLAB, which is used to collect data. Vibration responses of the Meriden Bridge are collected continuously (24/7) and an external 2 TB hard-drive is used to store the data. A remote internet connection is established with the desktop using Digi WAN 3G Wireless router from Sprint, which allows for remote access to the desktop.



**Figure 3.4: Cabinet containing Meriden Bridge system components**

### 3.3 Dynamic Truck Loading Tests

A total of three different data sets have been collected and will be referred to throughout the study. All data was collected using a sampling rate of 2048 Hz. A test was performed using a 5-axle loaded test truck of known characteristics in December of 2010. The vehicle travelled over Lanes 1 and 2 a total of 11 and 5 times, respectively. For the separate trials the vehicles travelled at constant speeds from 47 to 63 mph. The strain response due to each passing was matched with the corresponding run. The truck had a total GVW of 68,360 lbs and a length of 68 ft. An image of the vehicle can be seen in Figure 3.5.



**Figure 3.5: Test truck used in calibration**

Data collection of free flowing traffic was performed over three days in June of 2013. Each day contained a different number of vibration sets, with strain sensors running for a total of 2 minutes for each set. The trucks which passed over the instrumented bridge were later weighed using static scales at a near-by weigh station. Strain responses of the bridge were matched with the corresponding trucks. Figure 3.6 shows strain responses from Girder 6 during a period of two

minutes. From this particular string of data seven trucks have been identified by the system and their GVWs and speeds have been estimated.

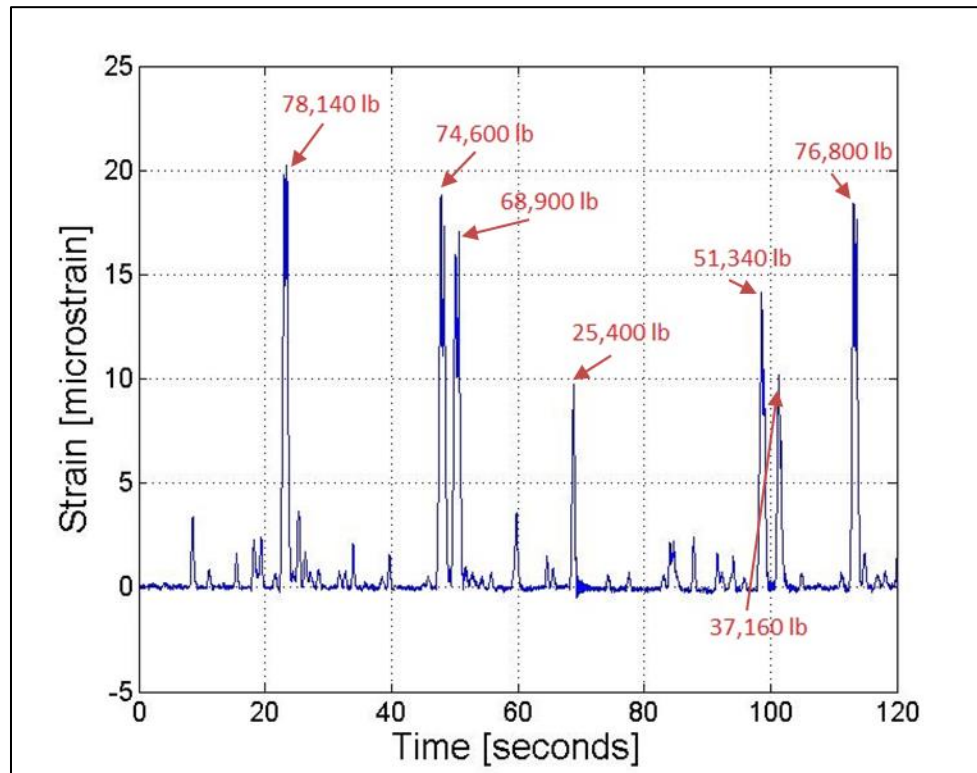


**Figure 3.6: Girder 6 strain responses during two minutes**

### 3.4 Long-term Data Collection

Meriden Bridge data was also collected continuously for a period of close to one year. Every hour, 10 strings of 5 minute data have been collected. These data files contain information from 14 out of the 48 available sensors, and include the sensors needed for this methodology. An additional 5 minute string of all 48 sensors were also collected in between every 10 strings. In this manner, about 95% of all possible strain data is collected with some delays occurring while the files are being saved and the algorithm is being reinitiated. A truck event is identified when a set strain value is exceeded; prompting the algorithm to examine all strain data 0.75 seconds

before and 1.75 seconds after the mentioned value. This setup has shown consistency in capturing strain data caused by a particular truck event.

Long-term traffic information has been collected since March of 2013. However, due to various issues with power, internet and sensor connections, and project continuation the records have been collected inconsistently. Table 3.1 shows the months during which data has been collected, the number of days of each month data was collected, percentage of data during the days it has been collected, and the percentage out of total data possible for the specific month. For example, for the month of March 2013 data was collected for 16 out of a possible 31 days. For these 16 days, 85% of possible strain data was collected, which results in 44% of data available for the entirety of this month.

**Table 3.1: Percentages of data collected per month**

<b>Month</b>	<b>Number of Days Collected</b>	<b>Percentage of Data for Days Collected</b>	<b>Percentage out of Total Data Possible per Month</b>
March 2013	16	85%	44%
April 2013	9	82%	25%
May 2013	17	64%	35%
June 2013	10	57%	19%
July 2013	10	89%	29%
August 2013	3	68%	7%
September 2013	21	80%	43%
October 2013	31	97%	97%
November 2013	30	98%	98%
December 2013	31	97%	97%
January 2014	26	93%	78%
February 2014	22	96%	76%
March 2014	31	95%	95%
April 2014	16	85%	45%
May 2014	30	91%	88%
June 2014	12	87%	35%
November 2014	20	61%	41%
December 2014	31	81%	81%
January 2015	30	87%	84%
February 2015	26	96%	89%

### 3.5 BWIM Methodology

This study uses one strain sensor per traffic lane to determine the speed and GVW of trucks passing over the instrumented bridge. Both sensors are located on the steel girders of the bridge and measure the vibration excitations of a specific girder located under a travel lane. This method uses the theory initially developed by the works of Ojio and Yamada (2002), and builds on the findings of Cardini and DeWolf (2007) and Wall (2009).

The developed theory uses the assumption that each girder under a lane behaves as a simply supported beam when exposed to a load from that specific lane. By instrumenting a girder directly under a highway lane, each axle of a vehicle can be assumed to act as a point load moving along the girder at a fixed spacing and a constant speed. This will make the vibration response caused by each moving truck to act like a group of point loads moving along a simply supported beam.

#### 3.5.1 Gross Vehicle Weight

The GVW is found by relating a known GVW from a calibration vehicle to the unknown GVW of a vehicle of interest. This method was developed by Ojio and Yamada (2002), and was used by Wall (2009). The GVW of an unknown truck can be determined by multiplying the influence area of an unknown truck times a calibration factor. This calibration factor is found by dividing the GVW of a known calibration truck over the influence area of that known truck, as shown in Eq. 1 (Wall, 2009).

$$\frac{A_k}{GVW_k} = \frac{A_u}{GVW_u} \quad (1)$$

where,  $GVW_k$  and  $GVW_u$  are GVW weights of known and unknown trucks, and  $A_k$  and  $A_u$  are influence areas for known and unknown trucks, respectively.



The ratio of the GVW of an known vehicle over the influence area can be defined as a calibration constant,  $\beta$ . By substituting this constant in Eq. 1 the relationship shown in Eq. 2 can be established.

$$GVW_u = A_u \beta \quad (2)$$

The influence area of a moving truck is a function of strain with respect to distance,  $\varepsilon(x)$ . This value can be modified to be with respect to time, by multiplying it by speed. This is shown in Eq.'s 3 and 4.

$$A(x) = \int_{-\infty}^{\infty} \varepsilon(x) dx \quad (3)$$

$$A(x) = v \int_{-\infty}^{\infty} \varepsilon(t) dt \quad (4)$$

Finally, the strain can be represented over discrete time intervals, as shown in Eq. 5,

$$A(x) = \frac{v \Delta t}{N} \sum_{i=1}^N \varepsilon(i \Delta t) \quad (5)$$

where,  $\Delta t$  is the discrete time interval, and  $N$  is the total number of measurements needed for the truck to cross the bridge.

### 3.5.2 Vehicle Speed Estimation

A vital step in the proposed method to accurately determine the GVW of a moving vehicle is to first correctly predict the vehicle's speed. The methodology in this study captures the peak in strain caused by the last axle of the vehicle being directly over the strain sensor and calculates the point in time the axle leaves the bridge. By knowing the distance between the strain sensor and the end of the bridge, and the time it took for the vehicle to travel this distance, the speed can

be estimated. An assumption is made that the truck travels at a constant velocity over this span. An approximate speed calculation can be made using the following equation:

$$v = \frac{L}{2t} \quad (6)$$

where,  $v$  (ft/s) is the average speed of the truck,  $L$  (ft) is the length of the bridge, and  $t$  (sec) is the time takes for the truck to get from mid-span of the bridge to the end. Figure 3.7 shows a typical strain response from a five-axle vehicle. An image of the truck that caused this response can be seen in Figure 3.8. From the strain response two clear peaks can be seen corresponding to the influence from the 2nd-3rd axles at approximately 56.9 seconds and 4th-5th axles at approximately 57.4 seconds. It can be seen from the image that a peak from the first axle at approximately 56.6 seconds is difficult to capture, which is why the methodology for speed calculation uses the end peaks rather than the first peaks. The last axle of trucks tends to be heavier for most cases leading to more consistent results.

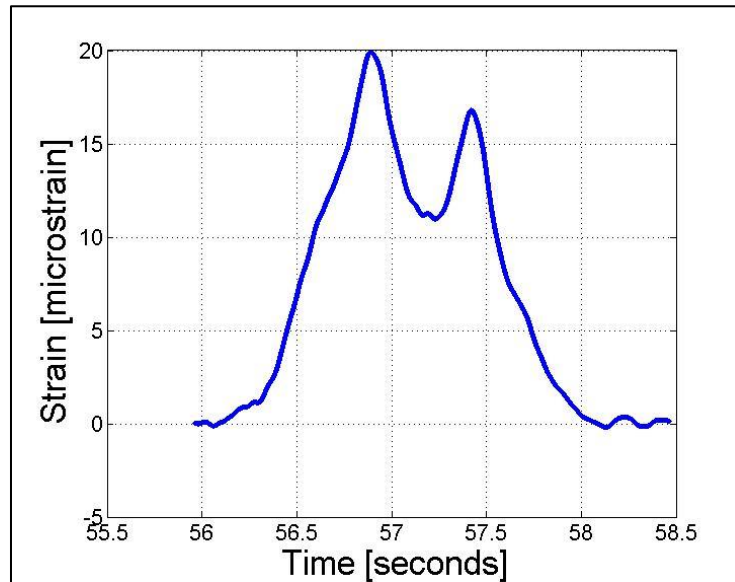


**Figure 3.7: Typical strain response due to a five axle truck**



**Figure 3.8: Typical five axle truck**

## **CHAPTER 4. BRIDGE WEIGH-IN-MOTION RESULTS**

In this chapter results are presented from the three data sets introduced previously. The GVW and speed calculations are examined for both lanes using the test trucks of known weight. The free flowing traffic data set is also analyzed from which the beta calibration factors are computed and accuracies of this algorithm are discussed. Analyses of various types of vehicles which result in speed miscalculations are discussed and strain responses as well as truck images are shown for each case. Equations of statistical parameters for GVW accuracy are presented and the results from the methodology are shown for all trucks, five-axle trucks, as well as trucks travelling in Lane 1 or 2. Long-term data results include an evaluation of speeds computed for weekdays or weekends and holidays. The information is presented for all months, the month of February 2015, as well as one day: February 13<sup>th</sup>, 2015. Furthermore the ADTT of the bridge for months containing more than 70% of all possible traffic data is estimated. To close, results for various types of speed errors which occur due to strain abnormalities from the long-term data set are presented.

### **4.1 Test Trucks Speed Calculation**

Data collection was performed on the bridge using a test truck. The vehicle performed a total of 16 runs over the bridge at a constant speed, 5 runs over Lane 2 and 11 runs over Lane 1. Greater details regarding this test can be found in Section 3.3.

The algorithm presented in this study has been applied to the strain responses of the test truck to examine the speed accuracy. Tables 4.1 and 4.2 show the actual speeds verses the calculated speeds for Lanes 1 and 2, respectively. Additionally a percent difference between the two calculations is presented. Two test runs were excluded from the validation of speed

calculations. During test run 2 in Lane 1, the strain response did not appear to match the type of response observed in previous trials. For test run 1 performed on Lane 2, the system was unable to calculate the vehicle speed because the strain response was not entirely captured.

It can be seen from the two tables that the percent difference between the actual and calculated speed is relatively accurate. The average percent differences for Lanes 1 and 2 were 0.08% and 3.38%, respectively.

**Table 4.1: Lane 1 test truck speed calculations**

Test Run Number	Actual Speed [mph]	Calculated Speed [mph]	Percent Difference
1	62	62.80	1.30
2	61	62.58	2.59
3	62	64.02	3.26
4	62	59.41	-4.17
5	62	62.73	1.18
6	63	64.89	2.99
7	55	52.40	-4.73
8	55	51.58	-6.22
9	49	45.65	-6.84
10	55	57.85	5.18
Average Percent Difference:			-0.08

**Table 4.2: Lane 2 test truck speed calculations**

Test Run Number	Actual Speed [mph]	Calculated Speed [mph]	Percent Difference
1	62	63.87	3.01
2	62	63.10	1.78
3	63	64.89	2.99
4	63	66.60	5.72
Average Percent Difference:			3.38

The GVW for the truck was determined from which a calibration  $\beta$  factor was computed. An optimal  $\beta$  value for each lane was determined using a trial and error, and the methodology presented in Section 4. The two factors were found to be  $\beta_1 = 0.0416 \frac{lb}{\mu\epsilon \times ft}$  for Lane 1 and  $\beta_2 = 0.0397 \frac{lb}{\mu\epsilon \times ft}$  for Lane 2. Tables 4.3 and 4.4 present the results for the test truck using the factors mentioned. The calculated GVW using the speed calculated from the methodology developed is found in the second column of both tables. The percent difference is based on the comparison with the weight of the test truck, which is 68.4 kips, and results of this are shown in column 3. Column 4 shows the percent difference using the actual speed presented in Tables 4.1 and 4.2, and the calibration factors are based on these values.

**Table 4.3: Lane 1 test truck GVW calculations**

Test Run Number	Calculated GVW [kips]	Percent Difference	Percent Difference with Exact Speed
1	66.81	-2.27	-3.52
2	66.24	-3.11	-5.55
3	65.82	-3.71	-6.75
4	63.93	-6.49	-2.41
5	64.46	-5.71	-6.81
6	65.35	-4.41	-7.19
7	71.66	4.83	10.04
8	71.55	4.66	11.60
9	67.81	-0.80	6.48
10	64.85	-5.14	-9.81
Average Percent Difference		-2.22	0.00

**Table 4.4: Lane 2 test truck GVW calculations**

Test Run Number	Calculated GVW [kips]	Percent Difference	Percent Difference with Exact Speed
1	80.24	17.38	13.95
2	59.06	-13.60	-15.11
3	63.42	-7.23	-9.93
4	80.30	17.46	11.11
	Average Percent Difference	2.80	0.00

## **4.2 Free Flowing Traffic**

The methodology discussed was further validated using strain responses of trucks from free flowing traffic. This test was used to establish an accuracy for the algorithm. A total of 190 trucks have been weighed right after passing the Meriden Bridge and a time stamp for each vehicle has been matched based on images from a camera.

Not all trucks were used to determine the accuracy of the algorithm. Certain truck events did not allow the system to correctly estimate the vehicle speeds or GVW. Such cases included trucks travelling over the bridge too slow due to a traffic jam, trucks changing lanes, multiple trucks on the bridge at the same time, trucks decelerating or accelerating excessively, and trucks that were very light. Out of the 190 vehicles mentioned, 25 trucks travelled during traffic, 3 changed lanes while crossing the bridge, 2 were effected by multiple presence of vehicles, and 5 trucks were considered very light. The algorithm registered another 16 cases as errors, due to either extensive acceleration, unusual vehicle configurations, or if the entire vehicle was not captured by the algorithm scheme. Each of the mentioned types of errors is discussed in this section. Examples of each case are presented.

#### 4.2.1 Trucks Travelling during Traffic Jams

The algorithm scheme captures strain responses of each truck for 2.5 seconds. This time frame was established to optimise capturing single vehicle events. The length of the Meriden Bridge is 85 ft and a point load can cross the entire bridge in 0.89 seconds travelling at 65 mph. A long truck with the length of 68 ft., such as the test truck mentioned in previous sections, would be able to cross the bridge in 1.60 seconds. However, were the 68 ft. long truck travelling at a speed of 40 mph, the entire truck would take 2.61 seconds to cross the bridge. This means that the entire strain response would not be captured and as a result the GVW would be miscalculated.

Figure 4.1 shows the strain response of a truck during a traffic jam. As can be seen from the image the vehicle's strain response is not captured. In such cases, the algorithm presented registers such vehicles as having a speed error, because the tail portion of the strain has not reached a value low enough for the truck to be considered entirely off the bridge. Figure 4.2 shows the image of the registered truck during traffic. Cars located close to each other in the distance can be seen confirming the congestion.

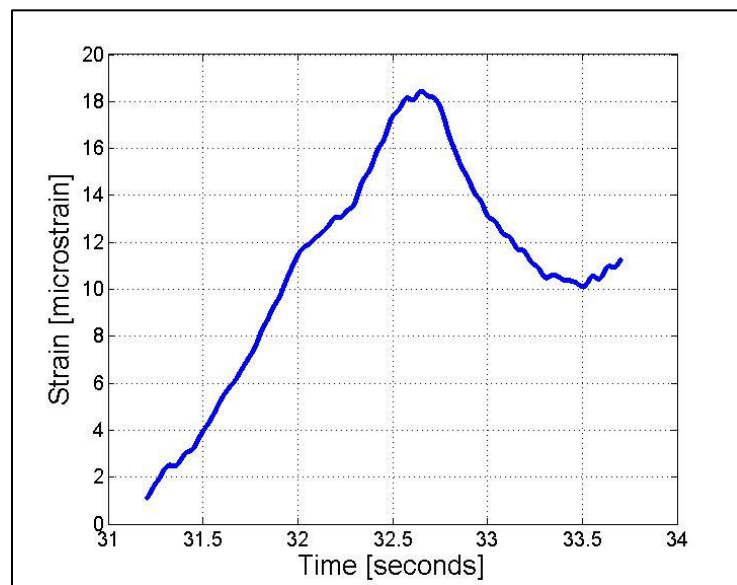


**Figure 4.1: Lane 1 strain response of a truck during traffic**





**Figure 4.2: Five axle truck during traffic**

#### **4.2.2 Lane Changes**

Trucks changing lanes, travelling in between two lanes or on the shoulder are rare. However, such cases do cause an underestimation of the GVW of the truck, since the strain of either Girder 4 or 6 will be lower than if the vehicle is travelling in one lane. This type of scenario is particularly difficult to identify, because the strain response appears similar to a normal strain response with the exception of large strains in the adjacent girder. Therefore, these types of cases cannot be identified by the algorithm. For the purpose of identifying the accuracy of the methodology the 3 cases during which lane changes occurred have been removed manually.

Figure 4.3 shows the strain response while a truck is travelling in two separate lanes at the same time. It can be seen in the image that the strain responses from Girders 4 and 6 are very similar, with Girder 6 having higher values. Figure 4.4 shows the five axle truck travelling over the bridge. In this figure it can be observed that the truck is travelling in between Lanes 1 and 2.

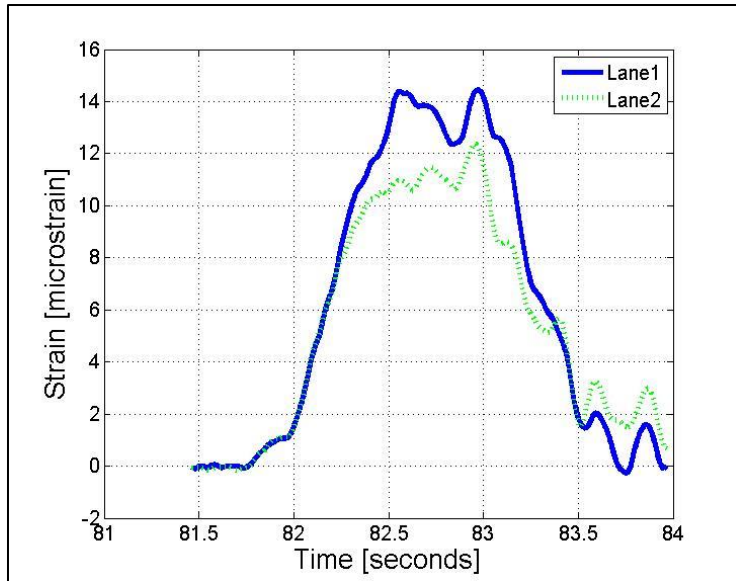


**Figure 4.3: Lanes 1 and 2 strain response of a truck changing lanes**



**Figure 4.4: Five axle truck changing lanes**

### 4.2.3 Multiple Presences

Multiple presence of trucks can affect the accuracy of the algorithm. If two trucks are side by side in two different lanes, the methodology will register only the truck which has a larger strain response. If two trucks are close together in the same lane it is possible for the strain response of both trucks to be combined. The algorithm usually is able to detect the latter case and identify an error, since it is possible for the last peak to be located at the end of the time frame. For the case of trucks being in parallel lanes, the algorithm is not able to distinguish that there is an issue since the response is similar to a normal strain response.

Figure 4.5 shows the strain response in Lane 1 due to two vehicles travelling closely together in the same lane. It can be seen from this image that the last peak in this response is at the very end of the time frame. Due to this the algorithm registers a speed error, since a speed cannot be estimated. Figure 4.6 shows the two vehicles which caused the strain response in Figure 4.5. A five axle truck can be seen being closely followed by a bus. Because the bus is close to the truck the 2.50 seconds time frame set for each vehicle is not sufficient to capture the strain from only one vehicle. The vehicle whose strain is between 85.3 seconds and 86.7 seconds is the five-axle truck, while the rise in strain after 87 seconds is caused by the bus.

A case where two trucks are travelling in parallel lanes at the same time has not been observed in this set of data and thus no figures of this case is provided.

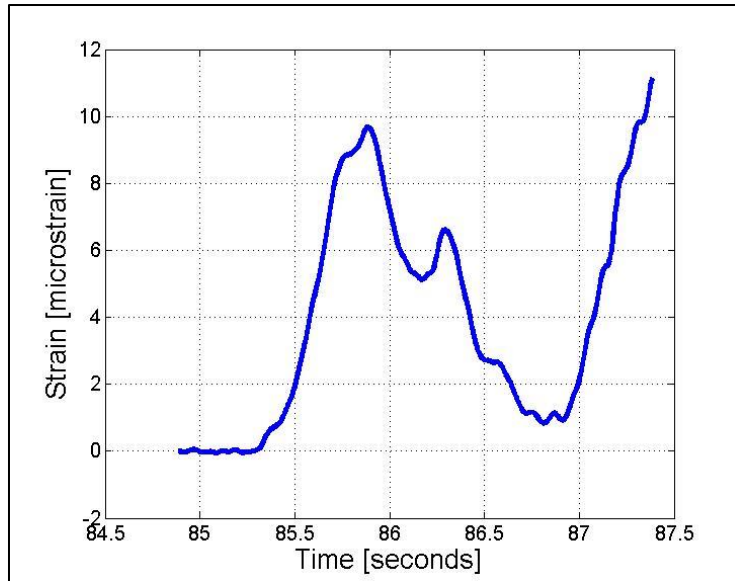


**Figure 4.5: Lane 1 strain response of a multiple presence event**



**Figure 4.6: Multiple presence event**

#### 4.2.4 Extensive Accelerations or Unusual Vehicle Configurations

The final category for truck miscalculations is the broadest one. Extensive accelerations, trucks slowing down or speeding up while crossing the bridge, can cause unusual vibrations on the bridge and do not agree with the original assumption that trucks are travelling at a constant speed. Due to these factors gross miscalculation of the truck speeds is possible. In order to avoid such cases, two upper limits have been set on the maximum speeds for both Lanes 1 and 2. In addition the algorithm accuracy can be compromised with unusual vehicle configurations, since the methodology was established for five axle trucks with consistent characteristics. This can lead to identifying a false strain peak as the last axle of the vehicle, or not correctly identifying when a vehicle is on the bridge. Regardless, a speed threshold is used to identify such cases.

Figure 4.7 shows the strain response of an irregular vehicle. In this particular case the correct peak corresponding to the last axle of the vehicle is difficult to identify, and the algorithm registered this vehicle travelling unreasonably fast. Figure 4.8 shows an image of the vehicle.

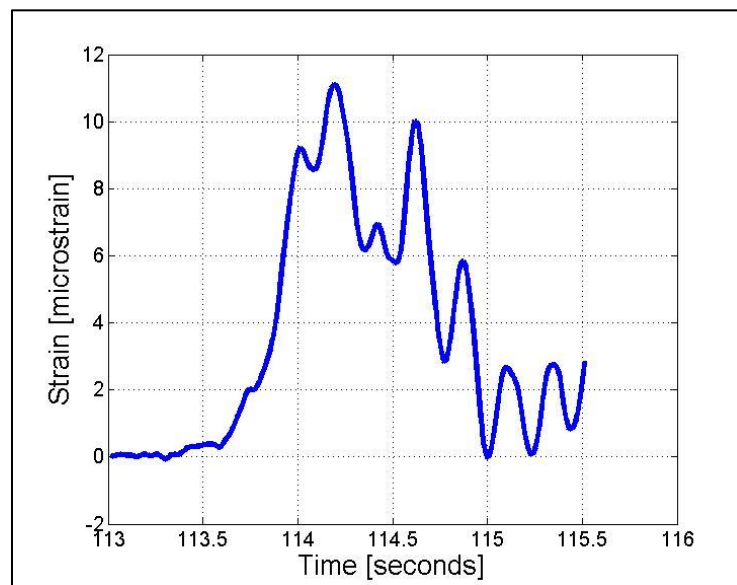


**Figure 4.7: Lane 1 strain response of an irregular vehicle**



**Figure 4.8: Irregular vehicle**

#### **4.2.5 Light Vehicles**

The algorithm did not perform well in determining the GVW of vehicles under the weight of 21 kips. A total of five examples of such vehicle have been recorded and all five samples had 2 axles. Three trucks were travelling in Lane 1 and two in Lane 2.

Out of the five identified light trucks, four of them were overestimated or underestimated by more than 20 percent. Due to this, it was established that the method presented does not support such light vehicles. The maximum legal GVW of a two axle truck in the state of Connecticut is 36 kips. It is extremely unlikely that two axle vehicles under 21 kips are to be overestimated by more than 60%, therefore if this system was used to assist with identification of overweight vehicles, it would not be of concern that it performs poorly for light vehicles. Figure 4.9 shows the strain response of a light vehicle travelling in Lane 1, while Figure 4.10 shows an image of the vehicle.

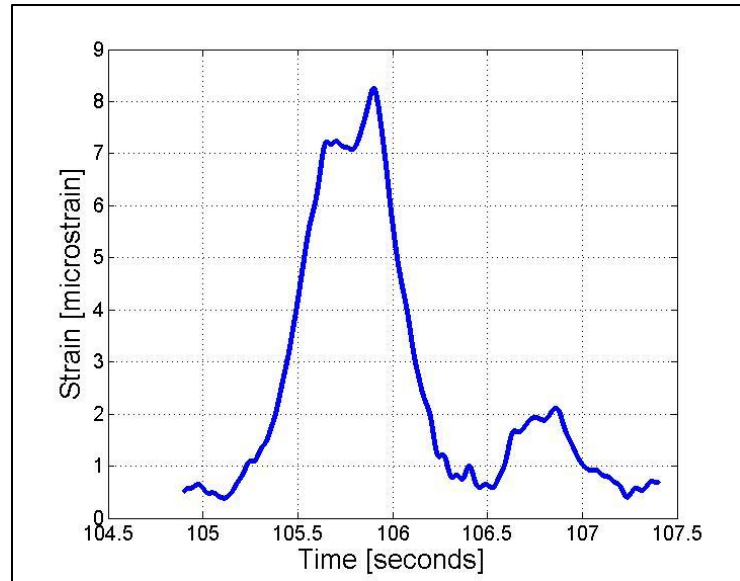


**Figure 4.9: Lane 1 strain response of a light vehicle**



**Figure 4.10: Light vehicle**

### 4.3 Free Flowing Traffic Evaluation

Out of the 190 weighed trucks, only 139 (73%) were used to validate the methodology. The mentioned cases due to traffic, multiple presence, and unusual vibrations have been identified by the algorithm automatically as errors. Eight total cases of trucks changing lanes as well as extremely light trucks have been removed manually. Out of these vehicles 133 travelled in Lane 1, while 6 travelled in Lane 2. In addition, 115 were five-axle trucks and 24 had more or less axles.

A minimum speed threshold has been set as 40 mph for both Lanes 1 and 2. As discussed previously, longer trucks would not be able to cross the bridge in the 2.5 seconds time frame and the strain would not be captured entirely. The thresholds of higher speeds were chosen as 90 mph for Lane 2 and 80 mph for Lane 1. Since the speed limit on the bridge is 65 mph, it was concluded unreasonable that a truck going in the central lane would be going faster than 25 mph over the speed limit, although possible. Similarly, it was deemed unreasonable that trucks would be travelling 15 mph over the speed limit in the slowest lane. For cases where the speed was estimated as an unreasonably low or high value, the truck event being analyzed was removed from the algorithm accuracy. This scheme works well for the majority of truck events.

### 4.4 Statistical evaluation of the algorithm

The accuracy of this algorithm is evaluated using both; the sample of trucks from test truck trials and 139 trucks from free flowing traffic. The GVW determined by the BWIM system is compared with the static weight. The calculation of GVW percent difference is shown in Eq. 7 such that,

$$E = \frac{(GVW_{BWIM} - GVW_{static})}{GVW_{static}} \times 100 \quad (7)$$



Where,  $GVW_{BWIM}$  is defined as the gross vehicle weight determined by the BWIM methodology,  $GVW_{static}$  is the gross vehicle weight determined by a static scale, and  $E$  is the calculated percent difference between BWIM and static measurements. Eq. 7 and  $E$  can be manipulated to calculate GVW difference in kips rather than percentage. Further both the GVW differences in kips and percent can be taken as an absolute value. These sets can be applied to the rest of the equations in this section.

The mean GVW difference in percent was determined as,

$$\bar{x} = \frac{1}{n} \sum_{i=1}^n E_i \quad (8)$$

Where  $E_i$  is the  $i^{th}$  vehicle GVW percent difference,  $n$  is the number of samples, and  $\bar{x}$  is the mean value for GVW percent difference. The mean GVW value was initially computed for all trucks using the calibration factor found from the test trucks. However, the mean from free-flowing traffic samples was not close to zero and so both  $\beta$  factors were adjusted for this data set. The newly found values are  $\beta_1 = 0.0389 \frac{lb}{\mu\epsilon*ft}$  for Lane 1 and  $\beta_2 = 0.0386 \frac{lb}{\mu\epsilon*ft}$  for Lane 2.

The GVW percent difference is assumed to act as a Gaussian distribution. In order to verify this, a Chi-square test was performed for the free-flowing traffic dataset. This test found that it is acceptable to assume these results behave as a normal distribution to a confidence of 90%. In addition to determining the mean value for GVW difference, it is also important to analyze the standard deviation of the sample. The standard deviation is defined as,

$$s = \sqrt{\frac{1}{(n-1)} \sum_{i=1}^n (E_i - \bar{x})^2} \quad (9)$$

Where,  $s$  is the standard deviation, and  $n$ ,  $\bar{x}$ , and  $E_i$  are defined previously.

The GVW percent difference is defined in terms of 95% confidence interval of difference, meaning that there is 95% confidence that the values fall within a range. Since the global mean is unknown and the amount of trucks used to evaluate the algorithm is limited, a t-distribution was used to evaluate the accuracy. The 95% confidence internal range for  $E$  can be seen in Eq. 10 using t-distribution:

$$\langle E \rangle_{t-\alpha} = \left[ \mu - t_{\frac{\alpha}{2}, n-1} \bar{x}; \mu + t_{\frac{\alpha}{2}, n-1} \bar{x} \right] \quad (10)$$

Where  $t_{\frac{\alpha}{2}, n-1}$  is the critical values of t distribution,  $n$  is the number of samples, and  $\alpha$  is the probability of Type 1 error. For example, by examining all trucks available, the number of samples would be  $n = 139$ , for a 95% confidence interval  $\alpha = 0.05$ , and  $t_{\frac{\alpha}{2}, n-1} = 1.978$ .

#### 4.5 Free Flowing Traffic Final Results

The GVW difference for the free flowing traffic can be seen in Table 4.5. The table presents the mean percent difference of GVW being calculated for both overestimated and underestimated values. An absolute mean and a standard deviation are also presented. All three values are shown for all 139 trucks, for five axle trucks, as well as for trucks travelling in Lanes 1 and 2. In column 1 the number of samples for each category is written in brackets.

**Table 4.5: Percentage GVW difference for free flowing traffic**

<b>Percentage GVW Difference</b>	mean [%]	absolute mean [%]	standard deviation [%]
All Truck [139]	-0.21	7.19	10.18
Five Axle Trucks [118]	-0.16	7.66	10.51
Trucks in Lane 1 [133]	-0.19	7.10	9.75
Trucks in Lane 2 [6]	-0.17	8.62	14.74

Apart from examining the GVW percent difference, the data can be further be examined by the difference in weight. Tables 4.6 presents this information in terms of GVW difference in kips rather than percent.

**Table 4.6: GVW difference for free flowing traffic in kips**

<b>GVW Difference in kips</b>	mean [kips]	absolute mean [kips]	standard deviation [kips]
All Truck [139]	-0.35	3.68	5.00
Five Axle Trucks [118]	-0.30	4.10	4.93
Trucks in Lane 1 [133]	-0.39	3.63	4.79
Trucks in Lane 2 [6]	0.45	4.44	7.57

Furthermore, the 95% confidence intervals for all types of trucks are presented in Table 4.7 in both percentage of GVW difference and kips.

**Table 4.7: 95% confidence interval accuracy**

<b>95% confidence interval ranges</b>	Percentage GVW difference	GVW difference [kips]
All Truck [139]	< -20.34 ; 19.92 >	< -10.26 ; 9.57 >
Five Axle Trucks [118]	< -20.98 ; 20.65 >	< -10.06 ; 9.46 >
Trucks in Lane 1 [133]	< -19.48 ; 19.09 >	< -9.87 ; 9.08 >
Trucks in Lane 2 [6]	< -36.25 ; 35.90 >	< -18.08 ; 18.99 >

The standard deviation for this methodology was found to be 10.18%. With this data it can be stated with a 95% confidence that trucks without unusual vibration characteristics will fall between -20.34% and 19.92%. These results are an improvement from previous studies done in 2009 with 127 trucks, which gave a standard deviation of 12.78% for Lane 1 and 19.72% for Lane 2 (Wall et al., 2009). If these accuracies were to be classified using COST 323

specifications the GVW for all truck and five-axle trucks would fall just short of a D+ (20) category and will be classified under D (25). The vehicles in Lane 1 will fall in the D+ (20) category. The number in parenthesis indicates the accuracy percentage for a 95% confidence. The vehicles in Lane 2 are unable to meet the lowest D (25) criteria. Since only 6 trucks are found in this lane results might be improved with more vehicle cases in this lane.

#### **4.6 Long-term Traffic Results**

The BWIM methodology for determining GVW and speed of trucks passing over the Meriden Bridge has been applied to continuous data collected since March 2013. Details regarding this data are presented in Section 3.4.

When examining all truck events which have been identified from the long-term data collection, the mean speed is found to be 63.1 mph with a standard deviation of 9.9 mph. It can be stated with a 95% confidence that all vehicle speeds will fall in the range of 43.7 mph and 82.5 mph. In addition, the mean speed for vehicles in Lane 1 is 60.4 mph with a standard deviation of 8.5 mph, and the mean speed for vehicles in Lane 2 is 65.9 mph with a standard deviation of 10.5 mph. These statistics result in 95% confidence ranges between 43.7 mph and 77.1 mph for vehicle speeds in Lane 1, and 45.5 mph and 86.4 mph for vehicles in Lane 2. Given the speed thresholds discussed in section 4.3, the ranges found for truck events in both lanes are reasonable, because the majority of registered truck events are close to the mean values which are similar to the speed limit on the bridge, 65 mph.

#### **4.6.1 Type of Data Collected**

From each individual day certain information has been stored and uploaded to a website accessible by representatives of CTDOT and researchers at the University of Connecticut. The information collected after processing the larger data sets consists of details regarding a time stamp, lane, speed, GVW, error, as well as strain responses for each truck event. Additionally, two accelerometer responses for each truck event are saved, but are not used in the current methodology.

For each truck event an exact time stamp is registered. This includes a matrix of 6 numbers saving a year, month, day, hour, minute, and second. The lane matrix involves a number of 1 or 2, depending on the lane in which the truck was travelling. This distinction is determined based on the strain values, meaning that out of the two girders under Lanes 1 and 2 the higher strain will indicate which lane the truck is in. The GVW and speed are based on the strain response under the identified lane.

#### **4.6.2 Monthly Speed**

The average speeds calculated for both Lanes 1 and 2 are presented in Table 4.8 for weekends and holidays, as well as weekdays. The average speeds are calculated per day and the average speed of all the days are then computed for each month, considering each day equally regardless of how much possible data is collected.

**Table 4.8: Monthly speed data**

<b>Month</b>	<b>Lane 1</b>		<b>Lane 2</b>	
	<b>Weekdays Average Speed</b>	<b>Weekends   Holidays Average Speed</b>	<b>Weekdays Average Speed</b>	<b>Weekends   Holidays Average Speed</b>
March 2013	59.10	59.82	64.39	64.91
April 2013	60.43	61.54	66.14	67.53
May 2013	60.85	62.12	66.66	67.13
June 2013	59.82	59.60	65.36	65.11
July 2013	61.72	60.42	68.33	66.67
August 2013	61.25	67.44	N/A	N/A
September 2013	60.05	59.99	66.12	66.36
October 2013	59.69	59.70	65.92	65.43
November 2013	59.48	60.53	65.21	65.97
December 2013	59.77	59.57	65.08	64.50
January 2014	61.79	61.17	67.65	66.76
February 2014	60.72	61.34	65.21	66.62
March 2014	60.44	60.62	66.00	65.99
April 2014	59.56	59.77	64.97	64.83
May 2014	60.04	61.22	65.68	66.73
June 2014	60.57	61.43	66.08	66.73
November 2014	59.32	60.18	64.59	65.79
December 2014	59.22	59.77	64.48	64.84
January 2015	61.80	61.27	66.95	66.68
February 2015	61.69	62.34	66.44	67.41

From this information it can be observed that the average monthly speeds for Lane 1 are between 59 and 63 mph for the two categories; weekends, and weekends and holidays. For Lane 2 the speeds are between 64 and 68 mph for both category days. The information presented does not account for the amount of data collected each month, nor the percentage of data collected for each day. Therefore, Table 3.4.1 should be consulted before making conclusions regarding the overall traffic speeds. This table presented the amount of data collected for each month and months which contain more than 75% of all possible data collected should be examined more

closely. Those months include: October, November, and December of 2013, January, February, March, May, December of 2014, and January and February of 2015.

#### **4.6.3 Speed Calculation: February 2015**

The month of February 2015 is examined individually to present the data in a different form. This month contained 96% of all possible data for 26 days, and an overall 89% of total data possible. Table 4.9 presents the average speeds for each day in February 2015. It can be observed in this table that the average speed in Lane 1 is between 52 and 64 mph and the average speed in Lane 2 between 52 and 70 mph. For all days the speed in Lane 2 is greater than that in Lane 1.

To validate the speed estimations the weather during this period is examined. The historical data in Meriden, CT has been looked into using the website “weather underground.” (Weather Underground, 2015). According to the website it snowed on multiple days during this month, but the days during which there was precipitation were February 2, 8, 9, and 26. The amount of snow precipitation from the four days was 0.28, 0.08, 0.10, and 0.01 inches, respectively. It can be observed that the average speeds were much lower than monthly average in the days mentioned. Particularly on February 2, 8, and 9 the speeds were the three lowest for this month, likely due to the snow which accumulated during this time.

This method of examining the data does not account for factors such as accidents or traffic delays not caused by weather. The speeds for February 2<sup>nd</sup> are unusually slow which could have been caused by factors other than weather, yet the largest snowfall occurred during this day.

**Table 4.9: Average speeds per day for February 2015**

<b>Day</b>	<b>Average Speed Lane 1 [mph]</b>	<b>Average Speed Lane 2 [mph]</b>
1-Feb	63.38	69.55
2-Feb	52.27	52.77
3-Feb	61.09	65.58
4-Feb	62.93	68.59
5-Feb	61.65	65.60
6-Feb	62.64	68.69
7-Feb	64.12	69.80
8-Feb	59.27	61.76
9-Feb	56.11	56.64
10-Feb	60.69	64.97
11-Feb	62.43	67.36
12-Feb	63.30	68.24
13-Feb	62.71	68.06
14-Feb	63.07	67.49
15-Feb	60.80	66.24
16-Feb	63.51	69.75
17-Feb	63.25	68.31
18-Feb	63.62	69.26
19-Feb	62.50	68.31
20-Feb	63.61	69.08
21-Feb	63.16	68.42
22-Feb	61.39	66.26
23-Feb	62.69	67.39
24-Feb	63.46	69.95
25-Feb	63.56	69.86
26-Feb	61.98	67.21
27-Feb	N/A	N/A
28-Feb	N/A	N/A

#### **4.6.4 Speed and GVW Calculation for February 13<sup>th</sup>, 2015**

The speed for a single day is further examined. The thresholds for Lane 1 are set between 40 and 80 mph, while the thresholds for Lane 2 are set between 40 and 90 mph. It is possible that the averages are significantly affected by the thresholds. Averaging the limits would present a mean



speed for Lanes 1 and 2 of 60 and 65 mph, respectively, and these numbers are close to the averages determined by the methodology presented.

February 13<sup>th</sup> was chosen to be examined individually, a day during which no unusual weather conditions were observed. The amount of truck events detected for this day is 4,813, including vehicles with speed errors. Figures 4.11 and 4.12 show histograms of truck speeds detected for individual truck events for Lanes 1 and 2, respectively. It can be seen from the two graphs that the most common speed is close to 65 mph for both Lanes 1 and 2. However, Lane 1 has almost as many trucks travelling in the 60 mph range and similarly Lane 2 has the second most truck travelling in the 70 mph range.

The truck GVWs for February 13, 2015 are also presented in a histogram form. Figures 4.13 and 4.14 show truck GVWs for Lanes 1 and 2, respectively. In Figure 4.13 two distinct truck event peaks can be observed at the 25 and 55 kips marks on the x-axis. To some degree these peaks represent unloaded and loaded vehicles and are a common observation in WIM truck data, while other factors also affect these larger peaks in truck events. The same peaks can be observed in Figure 4.14, with the 25 kips mark being significantly higher than any other observed vehicle weight category. This would physically draw the conclusion that lighter and larger unloaded trucks are more likely to travel in the middle lane, which is a reasonable conclusion. Similarly, from these graphs an overall observation can be made that heavier trucks tend to travel in the slow lane.

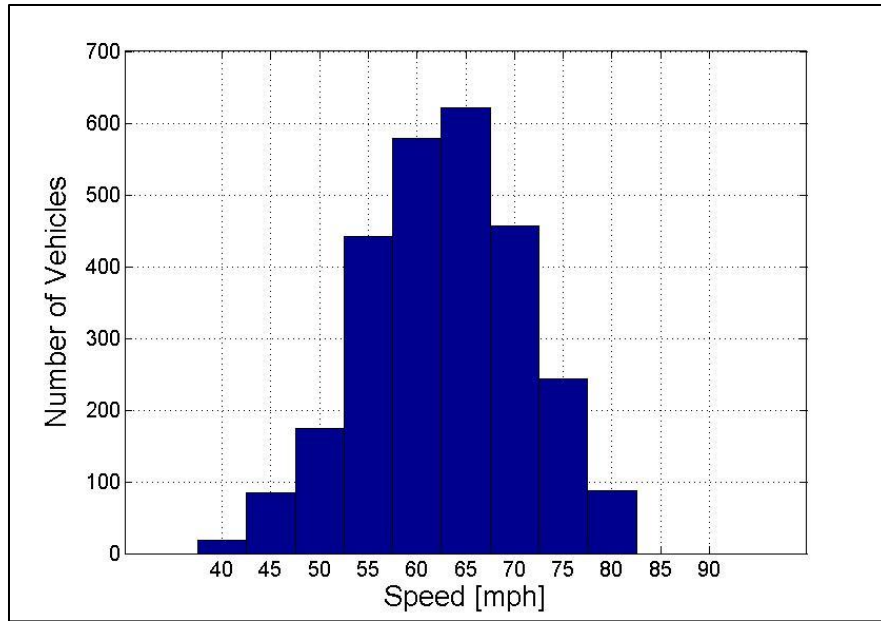


**Figure 4.11: Lane 1 traffic speeds**

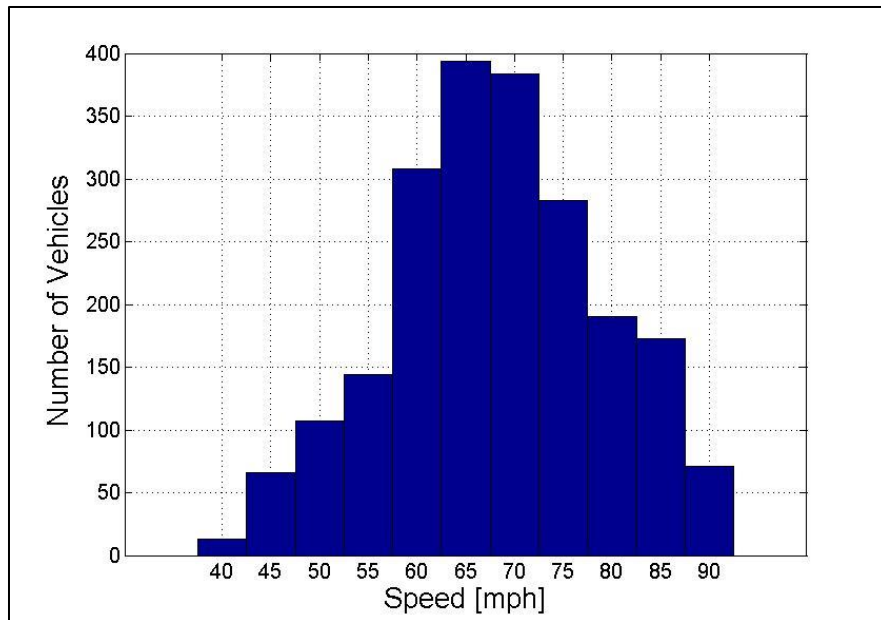


**Figure 4.12: Lane 2 traffic speeds**

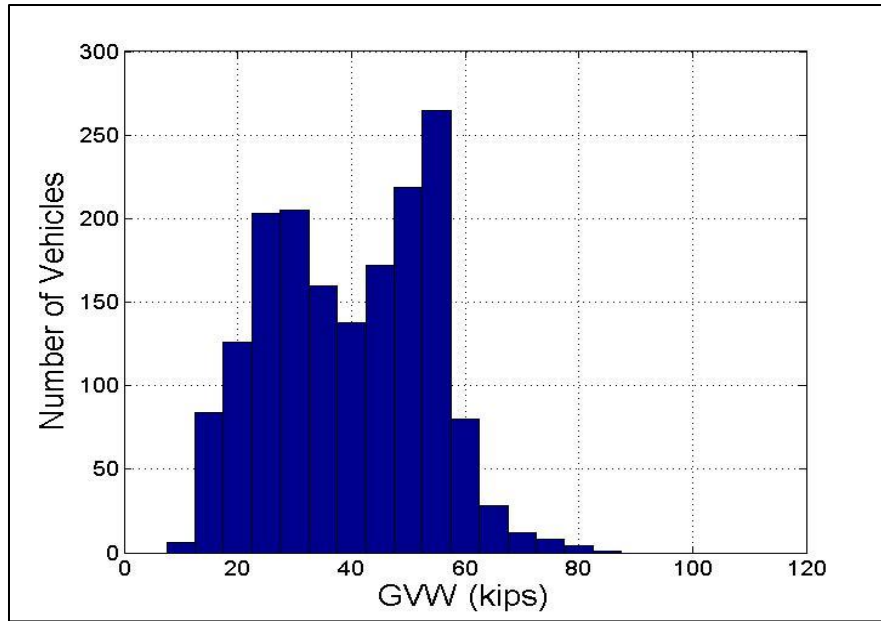


**Figure 4.13: Lane 1 GVWs**

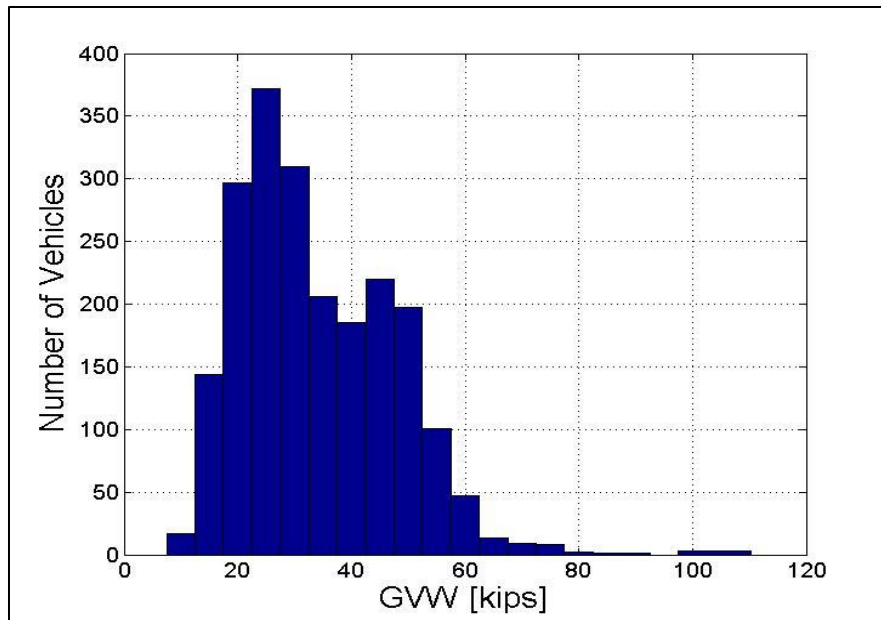


**Figure 4.14: Lane 2 GVWs**

#### **4.6.5 Average Daily Truck events**

The number of truck events registered by the BWIM system are presented. The events are computed for each day, after which all the days are averaged. If for a given day the entirety of data set is not collected, additional truck events are added based on a percentage of the missing data. For example, on January 3, 2014, the total truck events registered by the BWIM system were 1,718. However, since only 80 percent of possible data was collected for this particular day an extra 20% of the registered truck events were added, resulting in a total estimate of 2,067 trucks. Out this final amount an additional 10.95% is added to account for the capabilities of the BWIM system, which as discussed in previous chapters cannot collect the data for 24 hours. It takes about 7 seconds to save each 5 minute file of 14 sensors and 306 seconds to save five minute files consisting of all sensors. Therefore for every 50 minutes of data collected there is about a 6 minute gap. The final amount of trucks events for this day is 2,293.

This method of evaluating truck results can be misleading if a sufficient amount of data is not collected. Due to this the average daily truck events are only presented for months which contain more than 70% of data for the entirety of the month. A total of ten months contain this amount of data and are presented in Table 4.10. It can be seen that the Average Daily Truck Traffic (ADTT) is between 4,500 and 6,000 for all days. It should be noted that certain months are not represented in this table due to lack of data, including: April, June, July, August, and September. The two months which contain the largest amount of trucks are May and October, and it is likely that during the summer months larger amounts of freight is transported, since the construction industry is more active during this period. Consequently, months such as December, January, and February, are more likely to have a lower ADTT and these are most represented by the following data sets.

**Table 4.10: Average Daily Truck Traffic**

<b>Month</b>	<b>Average Weekdays ADTT</b>	<b>Average Weekend   Holidays ADTT</b>
October 2013	6002	2707
December 2013	5295	2345
January 2014	4581	2452
February 2014	5077	2727
March 2014	5480	2387
May 2014	6066	2510
December 2014	5405	2718
January 2015	4862	2425
February 2015	5257	2457

#### 4.6.6 Speed Errors

Multiple types of speed errors can occur with variation of the strain response. In section 4.2 some cases are discussed. Applying the error variation to a data set this large is more difficult and from the long-term data five different types of errors are identified and labelled with a particular number. An error value of 1, 2, 40, 80, or 90 is associated with each truck events where the speed cannot be accurately determined.

Type 1 errors occurred very rarely when the peak strain occurred at the end of the 2.5 second time frame and a car or small vehicle was in front of this peak. Such a case can be seen in Figure 4.13. Type 2 errors occurred when the last peak of a strain was detected, but the strain after it did not reach a value low enough for the truck to be considered off the bridge. Such a case could exist, because the vehicle was in a traffic delay or due to unusual vibrations. Figure 4.14 shows the strain response for such a case.

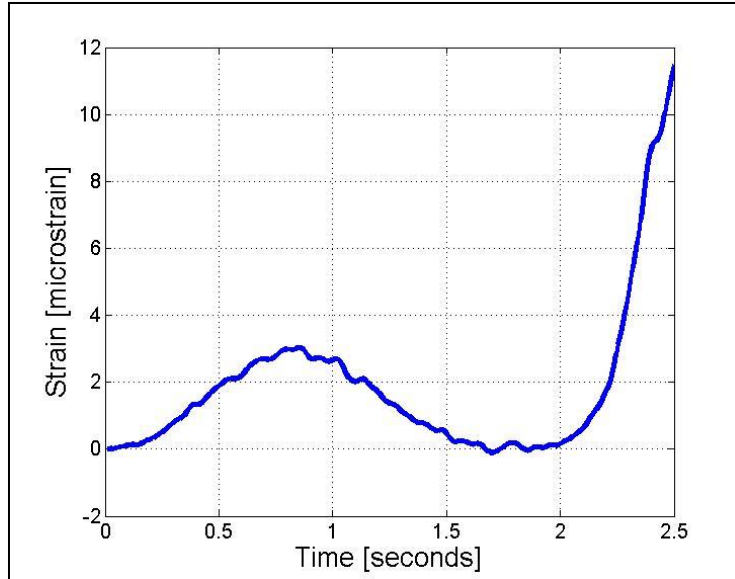


**Figure 4.15: Truck followed closely by light vehicle, Error Type I**

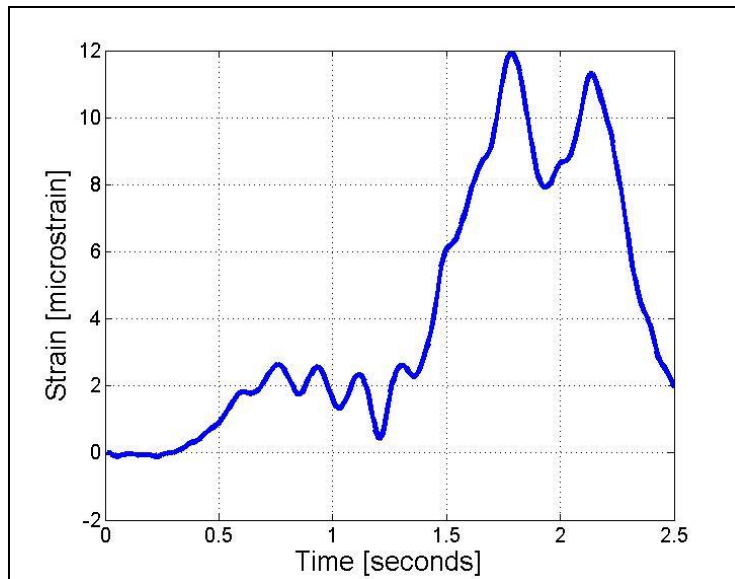


**Figure 4.16: Truck record not captured by algorithm, Error Type II**

Further types of errors include 40, 80, and 90. Type 40 error corresponds to vehicles travelling slower than 40 mph. Unlike Type 2 errors, an actual speed is calculated for Type 40 errors. This can result from a false peak being identified of as the last axle of the truck event.

Type 80 and 90 errors correspond to the speed in Lane 1 exceeding 80 mph and Lane 2 exceeding 90 mph. These types of errors can be caused by unusual vibrations due to large accelerations, resulting in a false peak being identified as the last axle of a truck. The five error categories presented do not account for two of possible errors discussed previously in Section 4.2, those being trucks changing lanes while crossing the bridge or errors due to light vehicles.

The amount of errors for each day will be discussed. Table 4.11 presents the average amount of errors of each month for both weekdays, and weekends and holidays. Additionally, the errors are presented as a percentage of total trucks.

**Table 4.11: Average percent errors**

<b>Month</b>	<b>Average Percent Error for Weekdays [%]</b>	<b>Average Percent Error for Weekends   Holidays [%]</b>
March 2013	18.60	9.74
April 2013	17.09	14.20
May 2013	17.96	12.92
June 2013	18.84	10.84
July 2013	18.44	13.05
August 2013	18.98	N/A
September 2013	20.13	12.71
October 2013	19.16	12.14
November 2013	20.99	11.73
December 2013	21.53	11.91
January 2014	19.06	11.53
February 2014	19.79	12.44
March 2014	18.09	10.48
April 2014	17.32	11.22
May 2014	18.51	11.58
June 2014	17.43	10.49
November 2014	18.26	12.96
December 2014	19.09	19.22
January 2015	18.58	14.70
February 2015	21.96	17.64

Table 4.12 shows the percentage of errors for each day in February, and type of errors observed. It can be stated from this table that Error Types 40, 80, and 90 contribute the most to the overall errors. By examining February 2, 8, and 9, during which snow has accumulated in the area, it can be noted that the type of Errors 80 and 90 are significantly lower when compared to Error 40 and Error 2 cases. This suggests that traffic delays have occurred during this day, a reasonable suggestion given the accumulation of snow.

**Table 4.12: Error types for the month of February 2015**

Day	Percentage of Errors	Error 1	Error 2	Error 40	Error 80	Error 90
1-Feb	11.76	4	6	53	91	73
2-Feb	31.99	1	182	297	127	67
3-Feb	18.79	11	86	278	232	213
4-Feb	17.61	11	57	287	271	267
5-Feb	21.43	22	106	423	254	277
6-Feb	21.24	10	50	318	350	309
7-Feb	17.46	8	25	116	186	127
8-Feb	13.07	1	37	93	50	41
9-Feb	19.62	2	159	420	118	125
10-Feb	16.37	11	33	316	169	196
11-Feb	19.83	17	65	344	278	323
12-Feb	19.18	24	61	307	317	299
13-Feb	21.32	13	57	332	278	346
14-Feb	20.46	3	40	146	118	126
15-Feb	15.01	6	37	37	61	31
16-Feb	20.06	8	32	189	253	266
17-Feb	20.65	12	41	261	279	293
18-Feb	22.15	14	68	290	347	377
19-Feb	21.77	21	58	351	346	357
20-Feb	22.95	7	46	283	430	314
21-Feb	23.65	3	34	171	163	159
22-Feb	19.65	0	26	148	98	74
23-Feb	34.09	15	88	519	466	459
24-Feb	21.94	13	44	280	390	355
25-Feb	20.29	22	37	282	357	317
26-Feb	24.13	7	45	226	236	222



#### 4.6.7 Temperature Effects on Algorithm Accuracy

The effects of temperature on the GVWs of truck events are examined, in order to ensure that changes in temperature do not have significant effect on the algorithm accuracy. The instrumented girders are made of steel, which deforms less at lower temperatures; therefore, some reduction in the algorithm accuracy is likely.

In order to study temperature effects the month of March 2015 is analyzed, which as can be seen from Table 3.1 contains 95% all possible truck data. Since temperature measurements are collected during five minutes of every hour as discussed in section 3.3, only a portion of the trucks found during this month can be evaluated. Figure 4.15 shows a scatter plot between temperature and GVW of individual trucks, represented by blue circles on the graph, for the month of March 2014. A line of best fit is plotted in red on the figure, which shows a positive correlation between temperature and GVW. The graph is only plotted for a GVW range of 10 to 80 kips, since a small amount of trucks are registered heavier than 80 kips.

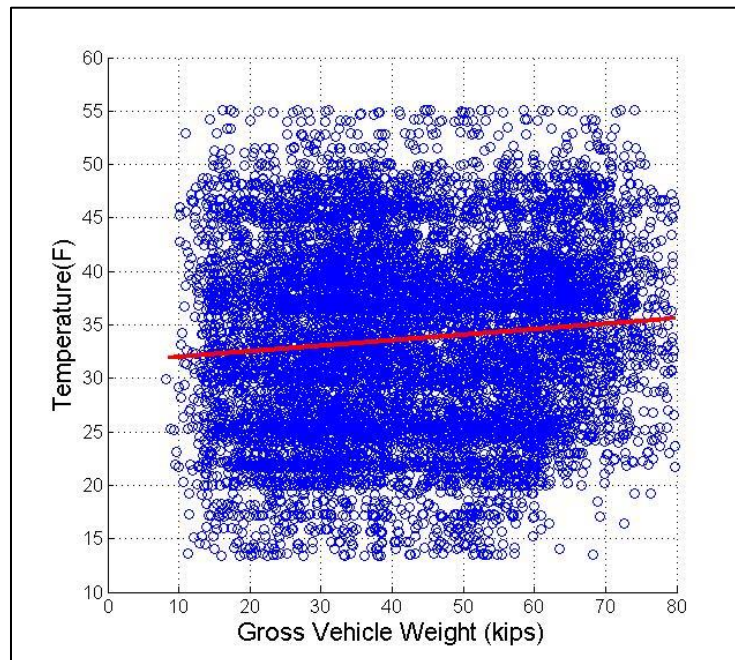


**Figure 4.17: Temperature and GVW correlation**

To estimate the temperature during a truck event the average of three of the four sensors instrumented on the bridge are taken, the fourth sensors having shown illogical results. A review of the website “weather underground” has shown that the temperature during March of 2014 has been in the range of 13 to 56 Fahrenheit for the city of Middletown (Weather Underground, 2015). This range matches the recorded temperature shown in Figure 4.15, which confirms that the temperature estimation from the sensors is reasonable.

A slight positive correlation is seen between GVW and temperature for March of 2014. The positive line of best fit goes from 32 Fahrenheit at 10 kips to 36 Fahrenheit at 80 kips. Since the range of temperature for this month was roughly 40 Fahrenheit, it is expected that this slope would be greater if the range was increased from 10 to 90 Fahrenheit, which are hypothetical temperatures that can be observed in the state of Connecticut throughout a year.

The correlation shown between temperature and GVW is not significant, but it is of value to account for this slope. It is possible that other factors play effects into this correlation. Hypothetically, vehicles travelling at night, when the temperature for this month was significantly lower, could be on average lighter than those travelling during the daytime.

## **CHAPTER 5. RELIABILITY STUDY RESULTS**

This chapter presents a reliability study that is conducted using the strain data collected from the Meriden Bridge. The strain responses of the instrumented bridge due to the test truck have been converted to equivalent positive moments and compared with the live and dead load moments on the bridge. The AASHTO LRFD codes have been calibrated for positive moment using the characteristics of the test bridge and strain responses from the center of two critical girders. Statistical parameters for moment resistance of steel-concrete composite bridges and dead loads are determined by review of previous research on this topic. The live load characteristics are found from long-term data collected for close to one year and compared with results from one month of data. A Monte Carlo simulation is performed to determine the most optimal live load factor for this bridge configuration.

### **5.1 Test Truck Results**

The data from the test truck trial discussed in Section 3.3 has been used to analyze the maximum strain caused by each pass on the two girders located directly under a travel lane. The maximum strain response due to each pass of the known truck has been examined in order to compare live load moment and the strain of the girder. Table 5.1 shows the maximum strain responses from each test run for both Girders 4 and 6, which are located underneath Lanes 2 and 1, respectively. The average strain response from the same vehicle is found to be 17.24  $\mu\epsilon$  for Girder 6 and 4.54  $\mu\epsilon$  for Girder 4. It can be observed from the table that the maximum strains for both girders are consistent apart from three cases, those being test numbers 2, 9, and 10. In the lane of interest the strain response is around 19  $\mu\epsilon$  for the three cases verses the 16  $\mu\epsilon$  for the remaining trials. This rise in strain is likely due to a dynamic effect or other vehicles, which have affected the girder during those three trials. During the tests the vehicle was travelling at a constant speed, so it is

assumed that the trials with lower values did not cause any impact excitation to the girders. As a result, the average of the eight cases is assumed to be the strain on the girder due to the truck without any dynamic effects, the value of which comes out to  $16.43 \mu\epsilon$ .

**Table 5.1: Strain responses from a Test Truck travelling in Lane 1**

Test Number	Speed [mph]	Girder 6 Maximum Strain [ $\mu\epsilon$ ]	Girder 4 Maximum Strain [ $\mu\epsilon$ ]
1	62	16.39	3.41
2	61	16.39	3.08
3	62	16.47	3.36
4	62	16.61	2.96
5	62	16.42	2.81
6	63	16.57	3.29
7	55	16.04	3.04
8	55	19.86	8.93
9	49	19.22	7.00
10	55	16.54	2.86
Average Strain		17.24	4.54

Similar information is presented in Table 5.2 for the test truck travelling in Lane 2. The average maximum strain for Girders 4 and 6 are found to be  $10.42 \mu\epsilon$  and  $8.84 \mu\epsilon$ , respectively. An abnormality is observed for the fifth test run where the strain in Girder 6 is higher than the strain in Girder 4. This is likely caused by a different truck travelling in the other lane and as a result this value has not been used in calculating the maximum average strain. It can be observed that unlike the test truck trials in Lane 1, passes of the truck in Lane 2 cause significantly lower strain responses in Girder 4, when compared to Girder 6 for passes in Lane 1. This difference is due to either the positioning of the two girders, or the location of the strain sensor.

**Table 5.2: Strain responses from a Test Truck travelling in Lane 2**

Test Number	Speed [mph]	Girder 4 Maximum Strain [ $\mu\epsilon$ ]	Girder 6 Maximum Strain [ $\mu\epsilon$ ]
1	62	11.25	8.25
2	62	9.14	8.72
3	63	10.16	8.50
4	63	10.63	14.59*
Average Strain		10.42	8.84

The strain responses from each girder are converted into equivalent live load moment through the following method. The maximum moment due to the test truck is found and compared with the maximum strain response from Girder 6 without a dynamic effect and multiplied with a load distribution factor (LDF) discussed in the next section. The results from Tables 5.1 and 5.2 have shown that Girder 6 receives the greatest strain and it can be concluded that the maximum LDF would apply for this girder. This girder is located almost directly under Lane 1 which is the slow lane and the most truck travelled lane on the bridge. It is therefore assumed that this girder will be the most critical of the entire bridge, as the loads from Lane 1 appear to affect it greatly as well as loading in Lane 2. A ratio is developed between the average strain calculated for the test truck times the LDF and the maximum moment calculated by passing the test truck over the bridge. The most critical LDF was computed for two truck cases, therefore the average maximum strain response observed on Girder 6 was added from Table 5.1 and Table 5.2.

## **5.2 Maximum Moment Calculations**

The AASHTO LRFD design equations use a LDF to convert the lane moment to per girder moment. The bridge in this study meets all the criteria to use this factor, including a girder spacing, thickness of slab, length of bridge, and longitudinal stiffness parameter ranges

(AASHTO, 2012). The maximum girder distribution factor is found to be 0.636. This factor is multiplied times the maximum moment found from the HL-93 design load for Strength I, which is a design truck HS20 and a distributed load of 0.64 k/ft.

The maximum moment due to dead load is calculated from the plans of the test bridge. This includes dead loads due to the concrete slab, an assumed wearing surface of 3 inches, and steel girders, plates, and diaphragms.

### **5.3 Statistical Parameters**

In order to conduct calibration of the live load factor statistical parameters for dead loads, live loads, and moment resistance need to be established. The statistical parameters for dead loads and moment resistance are determined through previous literature, while the live load factors are found through long-term data. The strain responses taken from the bridge already account for live load uncertainties due to multiple presence of vehicles and impact, so these types of statistical parameters are not be used.

#### **5.3.1 Dead Load Statistical Parameters**

Not much recent research has been conducted into determining the dead load statistical parameters. The parameters used in Nowak (1999) are based off NBS Report 577, which considers three different types of dead loads including: factory-made members (steel, precast concrete), cast-in place members (concrete), asphalt or wearing surface, and miscellaneous (Nowak, 1999). Table 5.3 presents the statistical parameters for the dead loads. The study presented is based on these factors.

**Table 5.3 Dead Load statistical parameters**

Dead Load Component	Bias Factor	Coefficient of Variation
Factory made	1.03	0.08
Cast-in-place	1.05	0.10
Wearing surface	1.00	0.25
Miscellaneous	1.03 -1.05	0.08 - 0.10

### 5.3.2 Moment Resistance Statistical Parameters

As was the case with the dead load parameters, the statistical parameters for resistance in this study are determined using the information provided in NCHRP Report 368. Literature on the topic suggests that there have been multiple improvements in the concrete and steel properties due to better control of material manufacturing (Kwon et al. 2009). However, the Meriden Bridge was built in 1964 and the NCHRP Report 368 data is from the year 1980, therefore the statistical parameters in the report are appropriate. Table 5.4 displays the moment resistance statistical parameters for material, professional, and resistance factors.

**Table 5.4: Moment Resistance statistical parameters (Kwon et al. 2009)**

Material/Fabrication		Professional		Resistance	
Bias	COV	Bias	COV	Bias	COV
1.07	0.08	1.05	0.06	1.12	0.10

### 5.3.3 Extreme Type I Modeling for Live Loads

The live load effects are modeled using Gumbel distribution, which is a type of extreme value distribution used to model highly unusual events. The design life of bridges in AASHTO LRFD methodology is based on 75 years, therefore maximum load effects are to be modeled keeping this time frame in mind. An assumption is made that the maximum truck event for each day has a

probabilistic distribution and that the largest maximum truck events for each day follow a Gumbel Type I distribution. A similar assumption is followed by Kwon (2009) and the reader may wish to examine this reference for more details. Days which have a larger maximum peak greater than 40  $\mu\epsilon$  have been used to establish statistical parameters for modeling the live load. Varying this peak value has shown similar results for long-term predictions and similar conclusions have been observed by Bhattacharya (2005) (Bhattacharya et al, 2005). These live load parameters have been further modified by accounting for the LDF, which according to Nowak has a bias value of 1.0 and a coefficient of variation of 0.12 (Nowak, 1999).

The cumulative distribution function (CDF) for the method can be found in Equation 14.

$$F(x) = e^{-e^{-\left(\frac{x-\mu}{\alpha}\right)}} \quad (14)$$

where  $\alpha$  is the scale parameter,  $\mu$  is the location parameter, and  $x$  is a random variable. This equation can be manipulated to project distributions accounting for a longer period of time than the data available, such as using one year's worth of data to simulate the maximum effect for 75 years. This is shown in Equation 15

$$F_n(x) = e^{-e^{-\left(\frac{x-\mu_n}{\alpha_n}\right)}} \quad (15)$$

where  $\alpha_n$  is the same scale parameter as in Equation 14 and  $\mu_n$  can be seen in Equation 16.

$$\mu_n = \mu + \ln(N) \quad (16)$$

where  $N$  is the difference between the amount of data used between  $F(x)$  and  $F_n(x)$ , for example for simulating the maximum load on a bridge during its lifetime,  $N$  would equal 75 if  $F(x)$  is based off one year of data.

Peak strains from either Girder 4 or 6 are taken from each day resulting in 32 points. The location parameter and scale parameters are found to be 42.4403  $\mu\epsilon$  and 5.4038  $\mu\epsilon$ , respectively, and these values account for the uncertainties associated with the GDF.



## 5.4 Final Results

The final calibration is conducted using the equations below. Equation 17 is the limit state function, where  $R$  is a Random Variable (RV) for moment resistance,  $D$  is a RV for moment due to dead loads, and  $L$  is a RV for moment due to live loads.

$$g = R - D - L \quad (17)$$

Equation 18 is the design equation used in this study and is the load combination for the Strength I Limit state in the AASHTO LRFD Bridge Design specifications (AASHTO, 2012).

$$\phi Rn \geq 1.25DC + 1.5DW + 1.75(LL + IM) \quad (18)$$

where  $DC$  is the moment due to the self-weight of the structure,  $DW$  is the moment due to the wearing surface of the bridge (pavement),  $LL$  is the moment due to the HL-93 load case, and  $IM$  is the moment due to impact, which for moment is to be one-third of the  $LL$  specifically for the fictional truck or tandem case and not the lane load.

The calibration of the live load factor is performed using a Monte Carlo simulation. The values of 1.25 and 1.50 in Equation 4 are kept constant. In addition, the  $\phi$  value is defined as 1.0 as appropriate for this bridge and is kept constant. The live load factor in the above equation (1.75) is assumed with a range of values from 1.0 to 2.0. With these values, a new  $Rn$  is calculated based on the defined factors and the known nominal live and dead loads. From these equations the probability of failure and a target reliability index can be determined by generating random variables and plugging them into Equation 17. The desired target reliability for AASHTO is 3.5, or 2 failures in 10,000 cases. This targeted index can be compared with the calculated reliability index from each assumed live load factor. Figures 5.1 and 5.2 show the square root of the difference between the targeted reliability index and the calculated reliability index plotted against the live load factor for the live load statistical parameters determine from

all data and the data for the month of May, 2014, respectively. The optimal values for the live load factor were to found to be 1.50 for all data and 1.65 for the data of May, 2014.

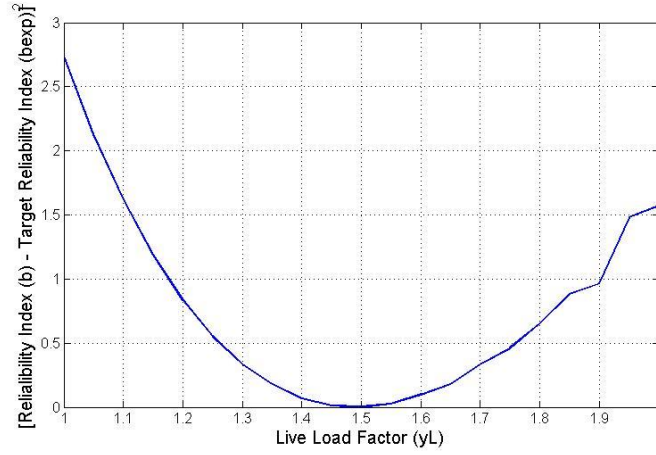


**Figure 5.1:  $(\beta_{resulting} - \beta_{target})^2$  vs. Live Load Factor using all data**

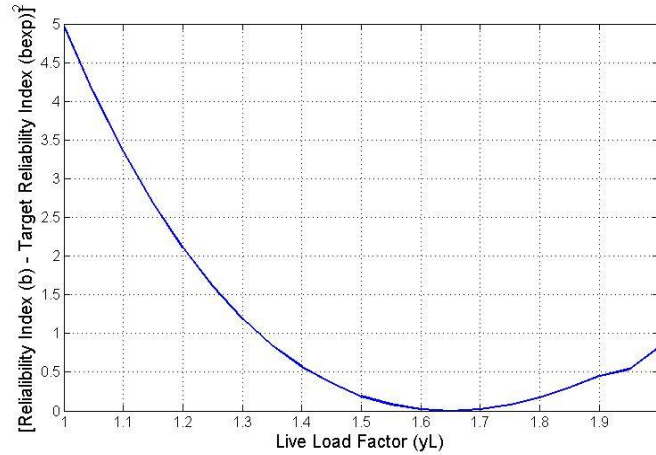


**Figure 5.2:  $(\beta_{resulting} - \beta_{target})^2$  vs. Live Load Factor using May, 2014 data**

#### 5.4.1 Dynamic Load Statistical Parameters

The dynamic load effect used in bridge design accounts for the condition of the road surface, the natural frequencies of the bridge, and vehicle dynamics (Nowak, 1999). The dynamic load effect is considered as an equivalent static load added to the truck loads and it has been shown constant

over time, when compared to static loads which increase as the weight of vehicle increase. This type of loading is accounted for by amplifying the HL-93 design truck by a factor of 1.33.

In this study the dynamic loadings on the Meriden Bridge are accounted for directly in the data, since the strain responses are taken from the bridge. When examining the applicability of this data set to different bridges in the state, the Meriden Bridge data accounts for the vehicle dynamics, but it does not account for road surface or bridge dynamics, which can vary from different bridges. This should be kept in mind when considering the application of the calibrated live load factor. The uncertainties of dynamic effects are defined in the NCHRP 368 have been added to the study for comparison. Since the most critical HL-93 case consists of two loaded lanes, the parameters used as defined by Nowak, 1999 are a bias factor of 0.10 and a coefficient of variation of 0.80. A live load factor of 1.65 is found using this method, but this value is overly conservative since as discussed all dynamic characteristics are accounted for in the data of the Meriden Bridge.

## **5.5 Study Application**

It is of interest to analyze how many bridges in Connecticut this factor can be applied to, given that the study involves local data from a bridge with specific characteristics. The factor cannot be applied to all types of bridges, such as concrete bridges for example. The test bridge in this study is a steel girder bridge, 85 ft. long, has as skew of  $11.5^\circ$ , and a girder spacing of 7'-3.5". Therefore, the calibrated factor can be applied to Connecticut steel girder highway bridges with less critical characteristics, including a shorter span, equivalent or better road surface conditions and smaller skew. It can be concluded by general literature that the bias factor is lower for shorter spans (Nowak, 1999; Kwon, 2009). This type of application assumes that all the bridges

are designed under AASHTO LRFD specifications or a more conservative methodology. Since the uncertainties of the girder spacing factors have been accounted for, the girder spacing will not matter for applications.

According to the National Bridge Inventory (NBI) there are a total of 4,219 bridges in Connecticut with 1,556 of those being stringer/multi-beam or girder highway bridges, such as the test bridge used in this study. Out of this sample, 1,045 bridges have a maximum span smaller than 85 ft, and an overall 435 bridges have a skew smaller than 11 degrees and a span shorter than 85 ft. Out of the remaining sample of bridges 66 have a rating of 4 or lower for the superstructure, and 157 have the rating 5. The 4 corresponds to “POOR CONDITION” meaning that there is advanced section loss, and the number 5 corresponds to “FAIR CONDITION” meaning that all primary structural elements have minor section loss (FHWA, 2012).

If section loss has occurred at the center of the bridge girders, where the maximum moment would be for a simple span bridge, a load rating analysis would be carried out to ensure the safety of the bridge with modified sections. The bridge rating factor (RF) is a ratio of bridge capacity over the live load capacity (FHWA, 2012). Equation 18 shows the calculation performed.

$$RF = \frac{\phi Rn - 1.25DC + 1.5DW}{\gamma L(LL + IM)} \quad (18)$$

where  $\gamma L$  is the evaluation live load factor and depends on whether an inventory, operating, or permit loading is being considered and the remaining factors have previously been defined. The new reduced factor would allow for a higher rating factor from the equation above. In addition, this factor can be used for moment capacities for new bridges in the state or bridge rehabilitation projects.

## **CHAPTER 6. CONCLUSIONS AND FUTURE WORK**

In this chapter conclusions are drawn regarding the BWIM and Reliability studies, involving a brief summary of the results. Lessons learned and recommendations for future studies are also presented.

### **6.1 BWIM**

A methodology for an existing BWIM system is presented and applied to three separate data sets including test trucks, free flowing traffic, and long-term traffic data. This methodology builds on findings from previous research and a new method is developed for calculating vehicle's speeds.

#### **6.1.1 BWIM Summary and Conclusions**

The test truck experiment demonstrated that the proposed algorithm can accurately predict vehicle speeds, however even if the speed is exact other factors can contribute to the inaccuracy of the algorithm. Applying this data to free flowing traffic has shown that the system can identify vehicle GVWs within a certain confidence interval. Various types of cases have been identified for which the methodology cannot function accurately and are organized in a list of errors. A unique contribution of this master's thesis has been applying this methodology to large traffic data-set consisting of 385 days. Applying the method to long-term traffic data has shown many details about the type of traffic on the bridge. Information has been provided regarding the average truck speeds on the bridge, the ADTT for certain months, as well as percentages for the amount of errors which occur for each month.

The type of data collected from long-term BWIM systems can be of extreme value to municipalities and managers of infrastructure. From the data used in this study, average speeds

as well as the ADTT travelling on the bridge for certain months have been determined. This information can be used to improve decisions regarding pavement and bridge design, and load rating analysis of bridges, as the ADTT is directly tied into those fields.

The GVW, speed, and time stamp of each identified truck has been saved and loaded to a website which can be accessed by representatives of the Connecticut Department of Transportation. Those reviewing the website are allowed to manipulate the data and draw general conclusions about the traffic pattern on the bridge. This can include identifying during which times the heavies' traffic travels or similarly when potentially overweight vehicles are travelling over the bridge. Through this information improvement in weigh station enforcements can be made.

### **6.1.2 BWIM Future Studies**

The current BWIM algorithm suffers from limitations which include not accounting for bridge or vehicle dynamic effects. Exploring these two vibrations could potentially improve the system accuracy to a considerable degree. Addressing this issue can improve both the speed and GVW calculations, as well as minimize the number of speed errors. The percent of errors due to inconsistencies in the strain is quite significant and can reach values higher than 25% for certain days. Some types of errors can be addressed to an extent, such as multiple presence of vehicle and vehicles travelling too slowly, however due to the variability of the data it is difficult to encompass all error types.

One motivation of BWIM systems is classification vehicle types, a type of information that has not been collected in this study. Methods have been explored of identifying peaks of the second derivative of strain, which corresponds to changes in the influence lines of tires.

However, this method was only able to distinguish between longer and shorter vehicles, and is inconsistent in detecting the number of axles. As mentioned in the literature review, recent studies have explored using wavelet analysis to identify the number of axles and this method has shown promise (Lechner, 2013; Bridgemon, 2014).

## **6.2 Reliability Study**

A study was conducted to calibrate the live load factor of the AASHTO LRFD Design equations using local data for the state of Connecticut.

### **6.2.1 Live Load Calibration Study Summary and Conclusions**

Strain responses from critical girders were taken and converted into moment, which in turn was used to estimate the worst moment the girders would experience using Extreme Type I distribution. Dead load and moment resistance parameters were taken from literature, while live load statistical parameters were calculated using strain responses from an in-service BWIM system. It was concluded from this study that the live load factor for moment resistance can be lowered from 1.75 to 1.50 for certain types of bridges.

The study performed has shown that the live load factor in the AASHTO LRFD Strength I design equation can be reduced based on traffic from a local Connecticut bridge. This evaluation of bridge capacity is of importance since costs associated with strengthening of bridges or rehabilitations are high and required if safety ratings are not satisfied. The study performed found that an estimated factor of 1.50 can be used to calibrate the positive moment factor for bridges in Connecticut with a length (85 ft.) and skew (11.5 degrees) lower than the

test bridge used in this study, not accounting for dynamic effects. Vibration effects encompass vehicle dynamics (suspension), bridge dynamics, and pavement conditions. This is accounted for in the data, but pavement conditions and bridge natural frequencies might vary for different bridges, and therefore a more conservative factor of 1.65 can be applied.

As discussed there are 66 bridges with a rating of the superstructure of 4 (Poor) or worst and 155 with a rating of 5 (Fair Condition) in the state of Connecticut, which would qualify for the new calibration factor. Bridges with low ratings require strengthening or complete replacements which can be very expensive. Application of this factor would allow management municipalities the ability to allocate funding for more critical projects.

### **6.2.2 Future Studies of Live Load Calibration**

The dual BWIM and SHM system presented was not intended to be used for the purpose of calibrating live load codes and some recommendations can be made for instrumentation of future bridges. Although it is assumed that the most critical girders have been instrumented with sensors, since Girders 4 and 6 are located very closely under respective lanes, it cannot be said with certainty that other girders are not more critical, such as Girder 5 located between both lanes. It would be ideal that all girders of a bridge be instrumented and the worst case can be determined. In addition, the sensors were located on the web right above the top flange. Since the maximum strain occurs on the bottom flange that would be a more optimal location for future instrumentation.

Further research interests include examining what kind of vehicle configurations cause the worst effect on the bridge, whether those are a single truck case or a multiple presence case, to better predict the long-term 75-year extreme event loadings. Additionally, it would be of value to find the neutral axis of the steel girder using the strain response from the top and bottom



flange and compute the maximum moment based on material laws. Using this procedure, moments due to vehicles would be computed directly from the bridge strain and there would be no need to use LDFs. However, this method would not be ideal in calibrating the AASHTO LRFD codes since the information from this bridge cannot be necessarily applied to all bridges in the state of Connecticut given that the difference in girder configuration will not be accounted for. Exploring the effects of natural frequencies on the moment would be of interest in analyzing the dynamic responses of the bridge.

## REFERENCES

- 2013 Report Card for America's Infrastructure. ASCE.  
<http://www.infrastructurereportcard.org/a/#p/bridges/overview>. Accessed April 12, 2014.
- AASHTO. *AASHTO LRFD Bridge Design Specifications*. 6<sup>th</sup> edition, 2012.
- Bell, E. S., Lefebvre, P. J., Sanayei, M., Brenner, B., Sipple, J. D., and Peddle, J. *Objective Load Rating of a Steel-Girder Bridge Using Structural Modeling and Health Monitoring*. ASCE Journal of Structural Engineering. Vol. 139, No. 10. 2013.
- Bhattacharya, B., Li, D., Chajes, M., and Hastings, J. *Reliability-Based Load and Resistance Factor Rating Using In-Service Data*. ASCE Journal of Bridge Engineering. Vol. 10, No. 5. 2005.
- Bridgemon. <http://bridgemon.zag.si/>. Accessed June 28, 2015.
- Brena, S.F., Jeffrey, A.E., and Civjan, S.A. *Evaluation of a Noncomposite Steel Girder Bridge through Live-Load Field Testing*. ASCE Journal of Bridge Engineering. Vol. 18. No.7. 2013.
- Cardini, A. J. and J. T. DeWolf. *Development of a Long-Term Bridge Weigh-In-Motion System for a Steel Girder Bridge in the Interstate Highway System*. University of Connecticut, 2007.
- Christenson, R., Motaref, S., McDonnell, A. *A Dual Purpose Bridge Monitoring and Weight-in-Motion System for a Steel Girder Bridge*. Proceedings of the International Conference on Weigh-In-Motion (ICWIM 6), 2012. pp. 397-408.
- Christenson, R., and McDonnell, A. *Advancing the State of Bridge Weigh-In-Motion for the Connecticut Transportation Network*. Transportation Research Board, SPR-2290. August 2, 2014.
- COST 323. *Weigh-in-Motion of Road Vehicles*. European WIM Specification – Final Report, Paris, 2002.
- FHWA. *Bridge Inspector's Manual*. Publication No. FHWA NHI 12-049. December, 2012.
- Fu, G. and van de Lindt, J.W. *LRFD Load Calibration for State of Michigan Trunkline Bridges*. Report RC-1466, Michigan Department of Transportation, MI, 2006.
- Guzda, M., Bhattacharya, B., and Mertz, D. *Probabilistic Characterization of Live Load Using Visual Counts and In-Service Strain Monitoring*. ASCE Journal of Bridge Engineering. Vol. 12, No. 1. 2007.
- HAKS Engineers P.C. *Bridge Safety Inspection, Bridge No. 03051*. 2012.

Jacob, B., and V. Feypell-de La Beaumelle. *Improving truck safety: Potential of weigh-in-motion technology*. IATSS Research, Vol. 34, 2010, pp. 9-15.

Kulicki, J. M., Prucz, Z., Clancy, M. C., Mertz, D. R., and Nowak A.S. *Updating the Calibration Report for AASHTO LRFD Code*. NCHRP Project 20-07. 2007.

Kwon, O.-S., Kim E., Orton, S., Salim, H., and Hazlett, T. *Calibration of the Live Load Factor in LRFD Design Guidelines*. Report No. OR11-003, Missouri Department of Transportation, 2009.

Lechner, B., Lieschnegg, M., Mariani, O., Pircher, M., and Fuchs, A. *A Wavelet-Based Bridge Weigh-in-Motion System*. International Journal on Smart Sensing and Intelligent Systems, Vol. 3, No. 4. 2010.

Lee, J., and G. Chow. *Dynamic Weight Threshold Control for Electronic Truck Screening Systems*. ITS in Daily Life. CD-ROM. The Intelligent Transportation Society of America, Washington D.C., 2009, pp. 15.

Li, Jingcheng. *Structural Health Monitoring of an In-Service Highway Bridge with Uncertainties*. Doctoral Dissertations. Paper 417. 2014.

Moses, F. *Weigh-in-Motion System Using Instrumented Bridges*. Transportation Engineering Journal of ASCE, 105 (TE3), 1979, pp. 233-249.

Nowak, A. S. *NCHRP Report 368: Calibration of LRFD Bridge Design Code*. Transportation Research Board, National Research Council, Washington, D.C., 1999.

Nowak, A. S., and Hong, Y.-K. *Bridge Live-Load Models*. ASCE Journal of Structural Engineering, Vol. 117, No. 9, 1991.

O'Brien, E., A. Znidaric, and A. Dempsey. *Comparison of Two Independently Developed Bridge Weigh-in-Motion Systems*. International Journal of Vehicle Design. Heavy Vehicle Systems, Vol. 6, 1999, pp. 147-161.

O'Brien, E., O'Donovan & Roughan. "Improving Bridge Weigh-in-Motion Technologies." 2014. <http://onlinepubs.trb.org/onlinepubs/conferences/2014/NATMEC/O'Brien-ImprovingBridgeWIM.pdf>. Accessed June 28, 2014.

Ojio, T. and K. Yamada. *Bridge Weigh-In-Motion Systems Using Stringers of Plate Girder Bridges*, Pre-Proceedings of the Third International Conference on Weigh-In-Motion, 2002, pp. 209-218.

SDDOT Briefing. *Truck Weights and Highways*. SDDOT Office of Research, 2003.

Strocko, Ed. *Data Opportunities and Challenges in Meeting MAP-21 Performance Measure Requirements*. TRB Plenary Session 2. June 11, 2013.

<http://onlinepubs.trb.org/onlinepubs/conferences/2013/MPO/Strocko.pdf>.

University Transportation Center for Alabama (UTCA). *Bridge Weigh-in-Motion (B-WIM) System Testing and Evaluation*. UTCA Report Number 07212. 2012.

Wall, C., Christenson, R., McDonnell, A.-M., and Jamalipour. *A Non-Intrusive Bridge Weigh-in-Motion System for a Single Span Steel Girder Bridge Using Only Strain Measurements*. Report No. CT-2251-3-09-5. Connecticut Department of Transportation, 2009.

WAVE. *Weigh-in-motion of Axles and Vehicles for Europe*. General Report, LCPC, 2001.

Weather Underground. <http://www.wunderground.com/history/>. Accessed June 28, 2015.